Inter-species comparison of life traits related to amnesic shellfish toxin kinetic in five pectinid species

Eline Le Moan, Laure Pecquerie, Laure Régnier-Brisson, Hélène Hégaret, Paulo F Lagos, Léo Heyer, Salvador Emilio Lluch-Cota, Fred Jean, Jonathan Flye-Sainte-Marie

Ecological Modelling 499 (2025) 110921

Contents lists available at ScienceDirect

Ecological Modelling

journal homepage: www.elsevier.com/locate/ecolmodel

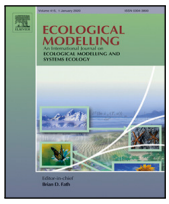

Inter-species comparison of life traits related to amnesic shellfish toxin kinetic in five pectinid species

Eline Le Moan [a,*], Laure Pecquerie [a], Laure Régnier-Brisson [b], Hélène Hégaret [a], Paulo F. Lagos [a], Léo Heyer [a], Salvador Emilio Lluch-Cota [c], Fred Jean [a], Jonathan Flye-Sainte-Marie [a]

[a] Univ Brest, IRD, CNRS, Ifremer, IUEM, 6539 LEMAR, Plouzane, F-29280, France
[b] Ifremer, Dyneco, LEBCO, Plouzane, F-29280, France
[c] CIBNOR, La Paz, 23000, Baja California Sur, Mexico

ARTICLE INFO

Keywords:
Pectinidae
Life-traits comparison
Amnesic Shellfish Poisoning
Dynamic Energy Budget theory
Multi-species parameter estimation

ABSTRACT

Pectinid species (scallops) hold significant economic value, but their filtration activity makes them vulnerable to harmful algal blooms, particularly *Pseudo-nitzschia* species producing domoic acid (DA). Domoic acid contamination can lead to amnesic shellfish poisoning in humans, causing prolonged fisheries closures and sales bans. This study aimed to compare several pectinid species to investigate if inter-specific differences in energetic traits could be linked to their ability to depurate the toxin. Using Dynamic Energy Budget (DEB) theory and the AmP multi-species estimation procedure, we analysed five species: two slow depurators (*Pecten maximus* and *Placopecten magellanicus*) and three hypothesised fast depurators (*Argopecten purpuratus*, *Mimachlamys varia*, and *Nodipecten subnodosus*). Results showed differences among species in assimilation rates, somatic maintenance rates, and reserve mobilisation rates but only the reserve mobilisation rates (*i.e.* the energy conductance parameter) consistently increased along the "slow-to-fast" depuration gradient. This research lays the groundwork for developing toxin kinetics models to quantify the processes affecting DA accumulation and depuration, and to assess the retention time of DA. Our approach and results will therefore not only be of interest to the DEB community in terms of multi-species approaches, but are likely to have applications in pectinid aquaculture and fisheries management.

1. Introduction

The Pectinidae family, ranks among the most extensively fished and cultured molluscs globally. The management of these resources represents a significant challenge for coastal countries due to their economic importance. Consequently, the closure of pectinid fisheries results in substantial economic losses. Over the past two decades, while mollusc aquaculture has seen a twofold increase worldwide, fisheries landings have remained steady (FAO 2020). This trend emphasises the growing importance of monitoring toxicity and risks associated with harmful algal blooms (HABs) (Hallegraeff et al., 2021).

Harmful algal blooms are natural phenomena characterised by the proliferation of microalgal species in localised environments. These blooms can be classified into three categories: microalgal species causing water discolouration and potential anoxia events, toxin-producing species affecting human health through the food chain, and species harmless to humans but harmful to marine organisms (Hallegraeff et al., 2004). Of particular concern are HABs producing toxins, representing the primary threat to pectinid fisheries. Pectinids, like bivalves in general, act as filter feeders, accumulating toxins produced by microalgae (MacDonald et al., 2016). When toxin levels surpass regulatory thresholds, fisheries are compelled to close.

Understanding the kinetics of toxins in pectinids is paramount for effective management during HABs, enabling the prediction of fishery closures and facilitating transitions to alternative activities or target species when feasible. Among the microalgal toxins, domoic acid (DA), primarily produced by diatoms of the genus *Pseudo-nitzschia*, stands out. Responsible for amnesic shellfish poisoning (ASP), DA, a water-soluble compound, was first detected in 1987 on Canadian coasts following mussel contamination (Wright et al., 1989). This toxin predominantly accumulates intracellularly into hepatopancreas of invertebrates. Pectinid species exhibit varying responses to DA, leading to differences in contamination levels and depuration rates (Álvarez et al., 2020; Blanco et al., 2002; Mafra Jr. et al., 2009; Wohlgeschaffen et al., 1992). However, for the moment toxicity of DA on pectinids has not been demonstrated (Liu et al., 2007).

* Corresponding author.
E-mail address: eline.lemoan@univ-brest.fr (E. Le Moan).

https://doi.org/10.1016/j.ecolmodel.2024.110921
Received 29 March 2024; Received in revised form 23 October 2024; Accepted 23 October 2024
Available online 19 November 2024

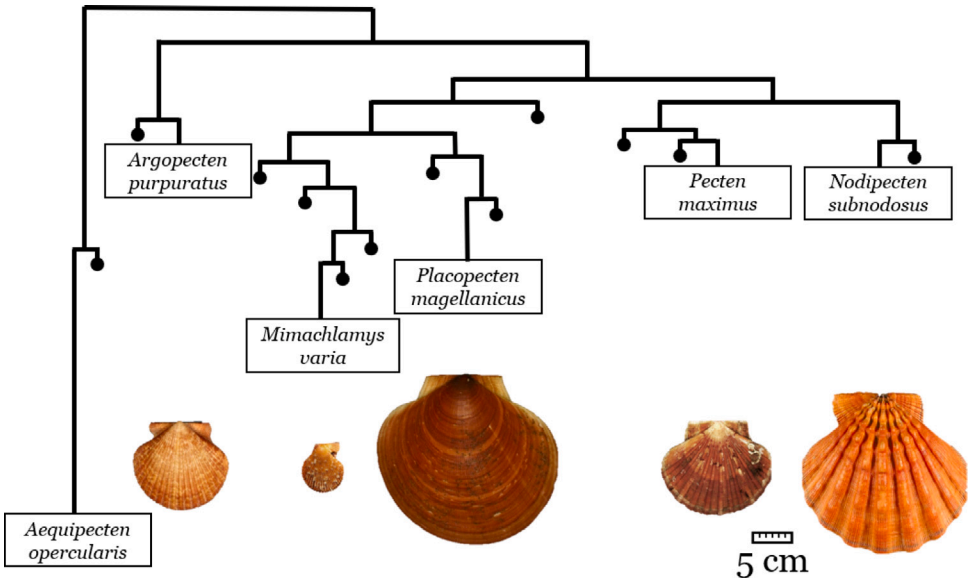

Fig. 1. Simplified tree of life based on genetic study of Saavedra and Peña (2006) with only species of interest. Species pictures, from WORMS website (World Register of Marine Species Ahyong et al., 2023), presented to scale to consider maximum shell height differences.

Pectinid species can be categorised based on their maximum contamination levels and depuration rates, ranging from "slow" to "fast depurators". For instance, the king scallop, *Pecten maximus* (Linnaeus, 1758) and the Atlantic deep-sea scallop, *Placopecten magellanicus* (Gmelin, 1791), exhibit slow depuration (Haya and Wildish, 1991; Douglas et al., 1997). Particularly, *P. maximus* accumulates high DA concentrations, especially in the digestive gland, with toxin persistence lasting from months to years (Blanco et al., 2002). Conversely, the Chilean scallop, *Argopecten purpuratus* (Lamarck, 1819), is considered to be a fast depurator, exhibiting rapid clearance of DA from its tissues following a contamination event, within a time frame of a few days (Álvarez et al., 2020). The variegated scallop, *Mimachlamys varia* (Linnaeus, 1758), and the giant lion's paw, *Nodipecten subnodosus* (G. B. Sowerby I, 1835) are hypothesised fast depurators based on expert knowledge and sanitary monitoring program for phycotoxins such as the REPHYTOX (2023) in France, for *M. varia*.

Despite hypotheses proposed to explain prolonged toxin retention in certain species, such as the absence of transfer between organs (Blanco et al., 2006), the absence of some membrane transporters in king scallops (Mauriz and Blanco, 2010), or the presence of autophagosomes and residual bodies that trap the toxin García-Corona et al. (2022), the underlying processes remain poorly understood. The retention of domoic acid is the result of a balance between toxin accumulation and depuration, both processes being species-specific (Blanco et al., 2020; Wohlgeschaffen et al., 1992). Hence, comparative studies between slow and fast depurators offer avenues to elucidate these mechanisms and fill existing knowledge gaps.

While monitoring natural contamination and decontamination in field settings and conducting *in-vivo* contamination experiments under controlled conditions pose technical challenges, investigating physiological similarities and differences among pectinid species within a unified conceptual and quantitative framework is feasible. Dynamic Energy Budget (DEB) theory provides such a framework, allowing for the comparison of species based on their DEB parameter values, which are closely linked to physiological traits. DEB models have been developed for numerous bivalve species, including pectinid species, for which parameters are available on the Add-my-Pet portal (AmP, 2023; Marques et al., 2018). Furthermore, DEB theory has already been successfully applied to study phycotoxins accumulation in a bivalve species (Pousse et al., 2019).

This study aims to investigate if one or several life traits drive the "slow" and "fast depurator" traits of pectinid species. A multi-species DEB parameter estimation was conducted as a first joint estimation of DEB parameters for five socio-economically important pectinid species for which (i) life traits data are available: *Argopecten purpuratus*, *Mimachlamys varia*, *Nodipecten subnodosus*, *Pecten maximus* and *Placopecten magellanicus* and (ii) DEB parameter sets for four of these species have been already estimated: *A. purpuratus*, *M. varia*, *P. maximus* and *P. magellanicus*. The aim was not to validate individual parameter sets for each species but to seek corroborating evidence to explain toxin kinetic differences. Given that the studied species belong to the same family, some physiological traits are expected to be similar between species, reflected by close DEB parameter values. In other words, we aim to (i) determine which parameter values can be considered similar between species and which ones differ, and (ii) how the differences in parameter values may relate to the depuration ability. The originality of the method is to compare five pectinid species in terms of life traits within the same conceptual and quantitative framework. We posit that a major part of life traits are similar across species, and thereafter introduce variations to reduce dissimilarities between observed data and model predictions. We hypothesise that assimilation rate should be higher for species with higher toxin concentrations and energy mobilisation rates and somatic maintenance costs should be higher for "fast depurator" species.

2. Materials and methods

2.1. Studied species and data collection

2.1.1. Species

Our study compares five pectinid species: the Chilean scallop, *Argopecten purpuratus* (Larmack, 1819), the variegated scallop, *Mimachlamys varia* (Linnaeus, 1758), the giant lion's paw, *Nodipecten subnodosus* (G. B. Sowerby I, 1835), the king scallop, *Pecten maximus* (Linnaeus, 1758) and the Atlantic deep-sea scallop, *Placopecten magellanicus* (Gmelin, 1791). Phylogenetically, *P. maximus* and *N. subnodosus* are the closest species, with *A. purpuratus* being more distantly related (Saavedra and Peña, 2006). A simplified phylogenetic representation of the species and their relative size are shown in Fig. 1. To minimise the impact of population differences, we selected only one region per species: Paracas Bay for *A. purpuratus*, Bay of Brest for *M. varia* and *P. maximus*, Gulf of California for *N. subnodosus* and Northeastern Canada for *P. magellanicus*. We determined typical temperature for each

Table 1
Life cycle data with age (defined from egg hatching) and shell height at life cycle transitions for the five pectinid species with their reference. Temperature at which data is given is defined in brackets. They correspond to zero-variate data used in the estimation.

Species	Age at D larva[a] (day)	Age at settlement[a] (day)	Age at 1st spawning[a] (day)	Life span[a] (year)	Height at D larva (cm)	Height at settlement (cm)	Height at spat (cm)	Height at 1st spawning (cm)	Ultimate height (cm)
A. purpuratus	2[b] (18 °C)	22[b] (18 °C)	62[c] (16 °C)	5[d] (16 °C)	0.008[b]	0.039[b]	0.7[q]	2[c]	11[e]
M. varia	2[f] (19.5 °C)	20[f] (18 °C)	272[g] (14 °C)	7[h] (16 °C)	0.0105[f]	0.0215[f]	0.1[f]	1.5[g]	7[g]
N. subnodosus	1[i] (26.5 °C)	15[j] (26.5 °C)	587[k] (24 °C)	7[e] (23 °C)	0.006[l]	0.0210[j]	0.3[r]	6.6[k]	19[e]
P. maximus	2[f] (18 °C)	27[f] (18 °C)	367[f] (13 °C)	20[m] (13 °C)	0.008[f]	0.15[f]	0.024[f]	4[f]	12[e]
P. magellanicus	4[n] (15 °C)	35[n] (15 °C)	364[o] (12 °C)	20[p] (12 °C)	0.0105[n]	0.035[n]	0.5[s]	4[o]	21[e]

[a] At given temperature in brackets (in °C).
[b] Farías et al. (1998).
[c] Aguirre-Velarde et al. (2019b).
[d] Stotz and González (1997).
[e] Minchin (2003).
[f] Breton et al. (Tinduff hatchery, pers.comm.).
[g] Régnier-Brisson (2024).
[h] Conan and Shafee (1978).
[i] Serrano-Guzmán et al. (1997).
[j] Angel-Dapa et al. (2015).
[k] Ramírez Arce (2009).
[l] Abasolo-Pacheco et al. (2009).
[m] Shumway and Parsons (2016).
[n] Culliney (1974).
[o] Parsons et al. (1992).
[p] MacDonald and Thompson (1985).
[q] von Brand et al. (2016).
[r] Mazon-Suastegui et al. (2011).
[s] Heasman et al. (2002).

species based on literature information and environmental conditions in these region. We analysed sea surface temperature from Modis-Aqua retrieved via the Giovanni online data system, developed and maintained by the NASA Goddard Eearth Sciences Data and Information Services Center (GES DISC). Consequently, typical temperatures were set at 8.5 °C for *P. magellanicus*, 12 °C for *P. maximus*, 13 °C for *M. varia*, 15 °C for *A. purpuratus* and 25 °C for *N. subnodosus*. Pectinids have a benthopelagic life cycle represented in Fig. 2A, starting with early life stages in the water column as embryos and larvae. They then undergo metamorphosis on the seabed, where they spend their juvenile and adult phases (Le Pennec et al., 2003). Due to the variations in the duration of these phases and in the behaviour of juveniles and adults across species, data on life history and eco-physiological traits were gathered for the five different species (Section 2.1.2).

2.1.2. Data collection

We conducted an exhaustive literature review to gather data on the life history and eco-physiological traits of the studied species. This included information on life stage transitions (*e.g.* age and shell size at first feeding, metamorphosis and first investment in reproduction), growth, body condition, reproduction and respiration. The life trait values at various life cycle transitions, along with the corresponding temperatures are summarised in Table 1.

For growth data, we used multiple datasets for each species: *in-situ* monitoring for *A. purpuratus* (Aguirre-Velarde et al., 2019b), *M. varia* (Régnier-Brisson, 2024) and *P. maximus* (EVECOS dataset from ‘‘Observatoire Marin de l’IUEM, INSU, Plouzané, found in Lavaud et al., 2017). For *N. subnodosus*, we used four datasets of shell heights at age (Racotta et al., 2003; Maldonado-Amparo et al., 2004; Arellano-Martínez et al., 2011; Ramírez Arce, 2009). For *P. magellanicus*, we included two studies conducted at different depths (10 m and 31 m) (MacDonald and Thompson, 1985; Roddick et al., 1994). Von Bertalanffy growth equation parameters were obtained for each species: *A. purpuratus* (Stotz and González, 1997), *M. varia* (Conan and Shafee, 1978), *N. subnodosus* (Villalejo-Fuerte et al., 2004), *P. maximus* (Buestel and Laurec, 1975) and *P. magellanicus* (Roddick et al., 1994). Weight-shell height relationships for *A. purpuratus* and *M. varia* were derived from the same *in-situ* monitoring data used for shell height at age (Aguirre-Velarde et al., 2019b; Régnier-Brisson, 2024). For *P. maximus*, due to the lack of data from the Bay of Brest, we used a dataset from a Galician population (Pazos et al., 1997). For *N. subnodosus*, we used wet weight at age (Ramírez Arce, 2009) and dry weight as a function of shell height (Carreño-León et al., 2023). Dry weight-shell height relationship for *P. magellanicus* was derived from Claereboudt et al. (1994). We retrieved egg diameter, number of eggs spawned per spawning event, and annual spawning frequency for each species, with values and references provided in Table 2. The number of oocytes served as a proxy for the number of eggs per spawning event, as data on spermatozoa number was unavailable. Respiration rate data were sourced from Aguirre-Velarde et al. (2016), Navarro et al. (2000) for *A. purpuratus*, from Shafee (1981), Shafee and Lucas (1982) for *M. varia*, from Purce et al. (2020) for *N. subnodosus*, from Artigaud et al. (2014) for *P. maximus* and from MacDonald and Thompson (1986) for *P. magellanicus*. These data were compared to model predictions.

2.1.3. Data standardisation to compare datasets

We compared life cycle data (Table 1) across species by calculating the mean, the standard deviation (mean ± sd), and the coefficient of variation (cv; $sd\ /\ mean$), expressed as a percentage. The following calculations were performed to facilitate the comparison and use of the data in the study.

(i) Growth The parameter t_0, in the von Bertalanffy growth equations, was estimated manually using data from other studies (Supp. Table. A.1). For *N. subnodosus*, fitting the von Bertalanffy growth curve from Villalejo-Fuerte et al. (2004) to continuous data from the four datasets used (Racotta et al., 2003; Maldonado-Amparo et al., 2004;

Table 2
Reproduction information for each species with references from literature. Mean value are given with minimum and maximum values in brackets and size of organism if available.

Species	Egg diameter (μrmm)	Oocytes spawned (# event^{-1})	Spawning events (# year^{-1})	Type of reproduction
A. purpuratus	61.8 (52 – 70)[a,b]	1,600,000[b] at 9.5 cm	15[b,c]	Simultaneous hermaphrodite[d]
M. varia	60[e]	4,000,000[e] at 5.5 cm	2[e]	Successive hermaphrodite[e,f]
N. subnodosus	52.5 (45 – 61)[j,k]	20,500,000[l] at 10 cm	1.5[j,k]	Simultaneous hermaphrodite[k]
P. maximus	65 (62 – 70)[g,h]	5,640,000[g] at 9 cm	2[g]	Simultaneous hermaphrodite[e,i]
P. magellanicus	66.8 (64 – 73)[m,n,o,p]	67,000,000[m] at 12.3 cm	1[m]	Gonochoric (male or female)[q]

[a] Martínez and Pérez (2003).
[b] Crisóstomo et al. (2024).
[c] Aguirre-Velarde (2016).
[d] Avendaño (2001).
[e] Breton et al. (Tinduff hatchery, pers.comm.).
[f] Perodou and Latrouite (1981).
[g] Paulet et al. (1988).
[h] Cochard and Devauchelle (1993).
[i] Priol (1930).
[j] Racotta et al. (2003).
[k] Angel-Dapa et al. (2015).
[l] Maldonado-Amparo et al. (2004).
[m] Langton et al. (1987).
[n] Culliney (1974).
[o] MacDonald and Thompson (1985).
[p] Carnegie (1994).
[q] Davidson (1998).

Arellano-Martínez et al., 2011; Ramírez Arce, 2009) was unsuccessful. We therefore fitted a new von Bertalanffy growth curve.

(ii) Reproduction Fecundity was calculated as the product of oocytes spawned per event and the number of spawning events. We identified three distinct reproductive strategies: gonochoric (either male or female gonads present throughout life: *P. magellanicus*), successive hermaphrodite (either male or female gonads present during the reproduction season but can change sex: *M. varia*) and simultaneous hermaphrodite (both male and female gonads present during the reproduction season: *A. purpuratus*, *N. subnodosus* and *P. maximus*). Data were available only for female individuals in all species. Thus, our analysis focused on females in gonochoric and successive hermaphrodite species. For simultaneous hermaphrodites, based on anatomical images (Blanco et al., 2020; Aguirre-Velarde, 2016; Maeda-Martínez and Lodeiros-Seijo, 2011), we assumed that the male gonad represents approximately one-third of the total gonad volume, and therefore, we adjusted the fecundity by multiplying the female fecundity by 1.5. The efficiency of gamete production (κ_R) was considered high for females due to the lipid-rich composition of fertilised eggs (Kooijman, 2010). Consequently, the efficiency of male gamete production was considered to be lower (Bodiguel et al., 2009). We hypothesised that the production of one male gamete requires twice the energy input compared to female. Therefore, we doubled the female defined fecundity to estimate the total energy input into the hermaphrodite gonad. Further details are provided in Supplementary Table A.4, and only results relevant to this hypothesis are presented and discussed below.

(iii) Allometric relationships We estimated allometric relationships between fecundity and shell height (Section 3.1.4), and between dry weight and shell height (Supp. Table A.2) by log-transforming variables and using linear regression analysis in R software (R. core team, 2022). Normality was assumed for sufficiently large datasets; otherwise, a Shapiro test assessed normality. Adjusted R^2 and p-value are provided in the text (Sections 3.1.3 and 3.1.4) or in supplementary materials (Supp. Table A.2). Relationships between dry weight and shell height were extrapolated from 0 to 12 cm for species comparison, corresponding to the size range of the five species. Respiration rates were derived from allometric relationships with dry weight or measured rates standardised by individual dry weight and converted to $mLO_2\ h^{-1}$ using the general gas equation if necessary. We examined respiration and growth rates at the typical temperature for each species and then converted these rates to the reference temperature used on AmP portal (20 °C) for interspecies comparison. This conversion applied the simple Arrhenius equation, with the Arrhenius temperature parameter set at 8000 K (Kooijman, 2010).

2.2. DEB theory, model and properties of physical co-variation

2.2.1. DEB theory

We compared the five species within the framework of Dynamic Energy Budget (DEB) theory (Kooijman, 2010). This theory quantifies the energy consumed by an individual and its allocation across physiological functions such as growth, maintenance, development and reproduction throughout its life cycle according to the environmental condition it encounters. Closely related species are modelled with the same equations but species-specific parameter sets. In summary, a DEB model describes the dynamics of four main compartments over an individual's life cycle: reserve (E), structural volume (V), maturity level (E_H) and reproduction buffer (E_R). Energy is first allocated to the reserve compartment through nutrition. A fixed fraction (κ) of this energy is then mobilised to support the structure compartment, while the remaining is directed to the maturity/reproduction branch. Maintenance is prioritised in both branches: somatic and maturity respectively. A schematic representation of the model is provided in Fig. 2B. The model incorporates two forcing variables: food and temperature and their impacts on physiological rates are modelled as a Holling type II functional response, and a simple Arrhenius function, respectively (see Tab. A.3).

2.2.2. DEB model

For pectinids, the standard DEB model is extended with the "*abj*" framework to include a type-$\mathcal{M}$ acceleration ("*a*"), characterised by

Table 3
Definition and equations used for observable variables from DEB state variables and parameters. Shape coefficient (δ_M) and energy cost of one egg (E_0) were estimated, thus values are defined in Table 4. Other parameters were equal for all estimations and species, density of structure, $d_V = 0.2\ g_{dw}\ cm^{-3}$, molar weight of reserve, $w_E = 23.9\ g\ mol^{-1}$, specific chemical potential of reserve, $\mu_E = 550{,}000\ J\ mol^{-1}$, fraction of reproduction energy fixed in eggs, $\kappa_R = 0.95$, η represent the matrix of coefficients that couple mass to energy flux, for details see Kooijman (2010) and the file 3_Theoretical_simulations/observables.m, from line 61, in repository https://github.com/ElineLM/LeMoanetal2024_Interspecies_comparison_ASP.

Observable trait	Symbol	Equation	Unit
Physical shell height	L	$V^{1/3}/\delta_M$	cm
Tissue dry weight	W_d	$d_V V + (E + E_R) w_E/\mu_E$	g_{dw}
Fecundity	F	$\kappa_R E_R/E_0$	# y^{-1}
Respiration rate	J_O	$\eta_{OA}\dot{p}_A + \eta_{OD}\dot{p}_D + \eta_{OG}\dot{p}_G$	mol O_2 h^{-1} ind^{-1}

increased assimilation and energy mobilisation during the larval stage; from birth ("*b*") to metamorphosis ("*j*") (Kooijman, 2014). During the embryonic stage, the organism relies on energy reserves for growth and development, as it does not feed. Birth ("*b*"), defined as the first feeding, marks the transition from embryo to larvae. Metamorphosis ("*j*") is defined as the shift to the juvenile stage, characterised by the end of metabolic acceleration. Upon reaching puberty ("*p*"), marking adult transition, individuals can feed, grow and reproduce, but development stops. The state variables of a DEB model are not directly observable. Observables quantities: shell height, wet weight, fecundity and respiration rates, are derived from conversion equations defined in Table 3, allowing for comparison between model predictions and observed data. The dynamics of the four compartments in the model are governed by differential equations based on energy flows; all model equations are detailed in Supp. Table A.3. In these equations, DEB parameters, which link compartments and fluxes, are estimated based on data and can be either general (applicable to many species) or species-specific. All parameters and Matlab codes are available in the repository https://github.com/ElineLM/LeMoanetal2024_Interspecies_comparison_ASP. In the text, we focus on parameters likely to vary between estimations and species, which are detailed in the Results section and listed in Table 4. Parameter values for a large number of species (4950 on 2024/09/20), including 10 pectinid species are accessible on the Add-my-Pet portal (AmP, 2023).

2.2.3. Physical co-variation rules in DEB theory

We compared the five species, by leveraging relationships between DEB parameters as implied by DEB theory. Specifically, some parameters and, consequently, life traits across species, are linked to their maximum size, known as "physical co-variation rules". Two DEB parameters co-vary with maximum size (Kooijman, 2010): the maximum surface-area specific assimilation rate ($\{\dot{p}_{Am}\}$) and the maturity threshold at puberty (E_H^p). The maximum surface-area specific assimilation rate, expressed in energy units per unit of structure per time, represents the highest rate of assimilation. The maturity threshold at puberty is the amount of energy required for the transition from juvenile to adult in DEB life cycle. These two parameters are placed on the energy flux where they are involved, on the DEB scheme (Fig. 2B) in orange. As described in Pecquerie et al. (2011) for salmon species, the standard DEB model incorporating physical co-variation rules can serve as a null model to compare species based solely on their maximum size. Species-specific variations in life traits can then be introduced to account for differences beyond those explained by maximum size alone.

2.3. Methodology

2.3.1. Individual parameter estimation

To develop a DEB model for a species, a specific set of parameters is required. The Add-my-Pet portal (AmP, 2023) provides parameter sets for *A. purpuratus*, *M. varia*, *P. maximus* and *P. magellanicus*, which we used as the basis for our study. However, we modified the data used for parameter estimation, to include new datasets or focus on specific regions and populations, as outlined in Section 2.1.1. For *M. varia*, we based our study on the one of Régnier-Brisson (2024), which provided

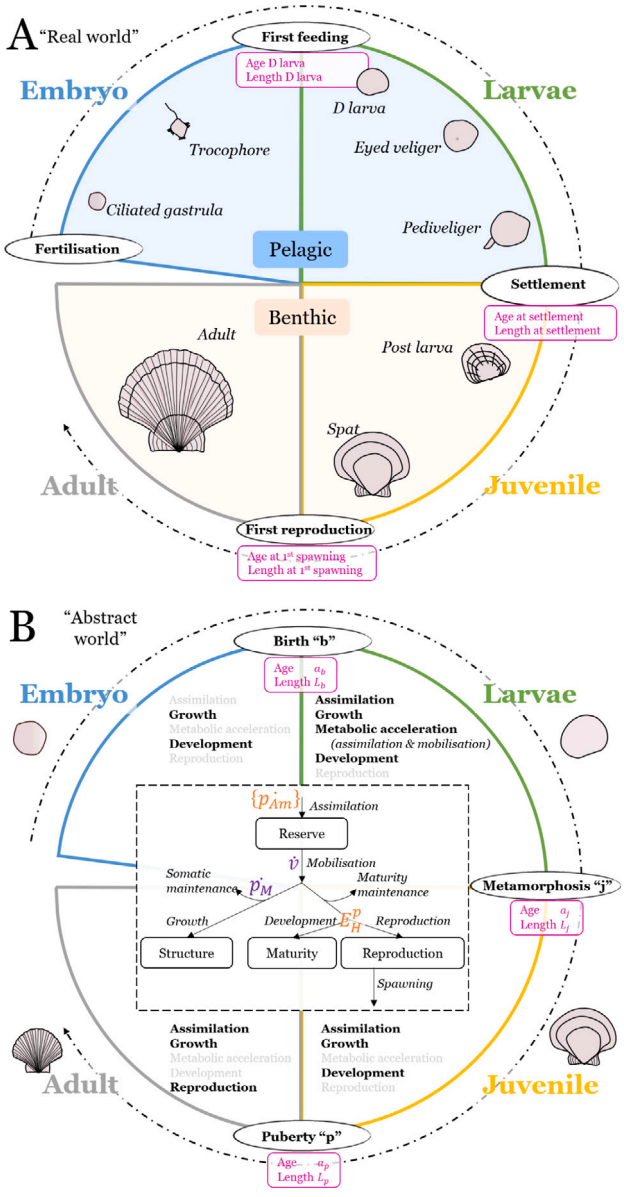

Fig. 2. Scheme of general life cycle for pectinid species named "real world" (A) and DEB model life cycle for pectinid, named "abstract world" (B). Transitions in pink in A are the ones used to define the DEB model life cycle in B. The specific features of each life stage are shown in B in each quarter, in bold black (if present) and transparent (if not present). The maintenance (somatic and maturity) occurs at each stage. Parameters in orange: maximum assimilation rate ($\{\dot{p}_{Am}\}$) and maturity threshold at puberty (E_H^p) represents the two parameters involved in the physical co-variation rules. Purple parameters: energy conductance ($\dot{v}$) and volume-specific somatic maintenance ($[\dot{p}_M]$) are the two parameters for which differences are included for the last multi-species parameter estimation.

a new set of parameters for this species. Furthermore, we estimated the parameters for *N. subnodosus* for the first time in this study.

We followed the parameter estimation procedure outlined on the AmP portal, using DEBtool and AmPtool Matlab software packages (DEBtool, 2022; AmPtool, 2022). Briefly, parameters were estimated simultaneously by minimising a loss function using the Nelder–Mead simplex method (Marques et al., 2018), based on the data provided for each species. The data used are of two types: zero-variate data (*i.e.* scalar values) and uni-variate data (*i.e.* vectors). Life-cycle traits are treated as zero-variate data, while growth in size and weight are considered as uni-variate data. Both types of data are defined at specific temperatures and levels of food availability. The goodness of fit is assessed using relative error (RE), mean relative error (MRE) and symmetric mean squared error ($SMSE$), with values ranging from 0 (perfect fit) to infinity, 0 to infinity and 0 to 1, respectively. For comparison, the mean errors (mean ± sd) for bivalves on the AmP portal are as follow: 0.10 ± 0.15 for MRE and 0.035 ± 0.068 for SMSE.

The standard estimation treats all data equally; however, weighting can be adjusted to emphasise or reduce the need to fit certain traits in the species dataset, as described in Meer et al. (2020). In this study, we increased the weight of ultimate shell height and annual reproductive effort by a factor of 10 to emphasise these traits. Conversely, due to challenges in estimating larval phase data alongside juvenile and adult data, we excluded larval uni-variate data and set the weight of larval zero-variate data (*i.e.* age, shell length and weight) at metamorphosis to zero, meaning these data were not included in the estimation procedure but are predicted for further model evaluation. Additionally, since the average water content of these pectinid species is around 80%–85% (Aguirre-Velarde et al., 2019b; DuPaul et al., 1989; Carreño-León et al., 2023), we adjusted the structure density (d_V) to 0.2 g_{dw} cm^{-3}, instead of the standard Bivalvia value of 0.09 used in the AmP parameter estimation procedure. The estimation involved two to four steps to balance the avoidance of local minima and computational time. Scripts are available on https://github.com/ElineLM/LeMoanetal2024_Interspecies_comparison_ASP.

2.3.2. Simulation based on P. magellanicus parameters

To determine whether all five pectinid species could be described by a single set of parameters following the physical co-variation rule, we tested the null model outlined in Section 2.2.3. We applied the DEB parameters of *P. magellanicus* to the five species under investigation, with *P. magellanicus* selected as the reference species due to its greater ultimate shell height. We only scaled $\{\dot{p}_{Am}\}$ and E_H^p parameters for each species according to DEB co-variation rules, based on their observed maximum length. We simulated individuals using the "*abj*" DEB model over an eight-year period, assuming one spawning event per year to represent annual cumulative reproductive effort. Due to limited data for larval and juvenile stages and the emphasis placed on toxin kinetics in exploited adults, we only considered the adult stage. All simulations were conducted under constant environmental conditions: abundant food and a reference temperature of 20 °C. The results are presented as shell height at age, tissue (dry or wet) weight, and annual fecundity as functions of shell height, along with respiration rate as a function of dry weight. For comparison between data and model predictions, we retrieved predicted annual fecundity at the closest shell height given in the fecundity data.

2.3.3. Multi-species parameter estimation

(i) Common estimation The multi-species parameter estimation procedure applied in this study follows the method outlined by Lika et al. (2020). Initially, we tested the null model described in Section 2.2.3 and applied in Section 2.3.2 using a common multi-species parameter estimation approach. This approach began with the initial parameter values of *P. magellanicus* with only $\{\dot{p}_{Am}\}$ and E_H^p differing between species, following physical co-variation rules. To simplify the process, the shape coefficient (used to convert physical measured length to volumetric length in DEB model) was fixed across all species, based on the average value from individual parameter estimations. This decision was made due to minimal observed differences in this parameter across species. We estimated nine parameters (z, $\dot{v}$, κ, $[\dot{p}_M]$, $[E_G]$, E_H^b, E_H^j, E_H^p and $\ddot{h}_a$) along with the scaled functional response for each of the 12 uni-variate datasets. The scaled functional responses were initially set at 1 for all uni-variate data, to avoid any pre-assumptions about regional food quality differences, and estimated during the procedure. Predictions and observed data for growth in shell height are presented in Fig. 5, while the results for growth in weight and weight-shell height relationships are provided in the supplementary material (Supp. Fig. B.1 and B.2).

(ii) Species-specific differences To enhance the accuracy of predictions for each species, we introduced species-specific differences by allowing two parameters to vary. The multi-species parameter estimation allows three types of relationships between species for each parameter: "equal" (the same value for all species), "different and independent" (a distinct value for each species), and "different and dependent" (distinct but close values between species). The degree of similarity between parameter values is incorporated into the loss function, with a higher degree of similarity resulting in closer values across species. For further details, see Lika et al. (2020). Contrary to the approach used in Lika et al. (2020) and Guillaumot et al. (2020), we introduced differences by allowing the volume-specific somatic maintenance ($[\dot{p}_M]$) and the energy conductance ($\dot{v}$) to vary between species, with degrees of similarity ranging from 0 (*i.e.* no difference between species) to 6 (*i.e.* high similarities between species). These two parameters are represented in purple in Fig. 2B, above the fluxes they modulate. Each estimation involved three runs and the MRE and SMSE were assessed for both individual and overall predictions. The final results of growth predictions in shell height at age, with degree of similarity of 6, are presented in Fig. 6, while the results for growth in weight and weight at shell height are provided in supplementary materials (Supp. Fig. C.1 and C.2).

3. Results

3.1. Patterns in observed life traits and simulations with P. magellanicus parameters

Table 1 summarises the life-cycle data obtained from the literature review for the five species, while Table 2 provides the information necessary to estimate the reproductive effort of each species. Fig. 3 presents the simulation results using physical co-variation rules as the null model (A–D), alongside the observed data (E–H) for shell height at age, dry weight, averaged annual fecundity as a function of shell height, and the relationship between respiration rates and shell height. Predictions of life-cycle data are shown in Table 5. When applying the parameters of *P. magellanicus* to the five species, we obtained a global MRE of 0.35 and a SMSE of 0.17. Specific errors (MRE and SMSE) are indicated in Fig. 4 as red points ("Simulation"). Notably, *N. subnodosus* and *A. purpuratus* exhibited the highest error values, while *P. magellanicus* and *M. varia* the lowest ones. As expected, the errors were higher than those from individual parameter estimation (green points).

3.1.1. Development

Despite a large difference in ultimate shell height, *M. varia* being the smallest (7 cm) and *P. magellanicus* the largest (21 cm), the age and shell length at birth and metamorphosis are relatively consistent across species. Birth (first feeding) occurs at approximately 80–100 µm ($L_b = 86 \pm 19$ µm, cv = 50 %) after 1 to 4 days-old ($a_b = 2.2 \pm 1.1\ d$, cv = 20 %) (Table 1). Metamorphosis takes place at a length between 200 and 350 µm ($L_j = 281 \pm 83$ µm, cv = 30 %), at 15 to 35 days-old ($a_j = 24 \pm 8\ d$, cv = 30 %) (Table 1). However, puberty (first maturity) shows more variation among species and appears to be

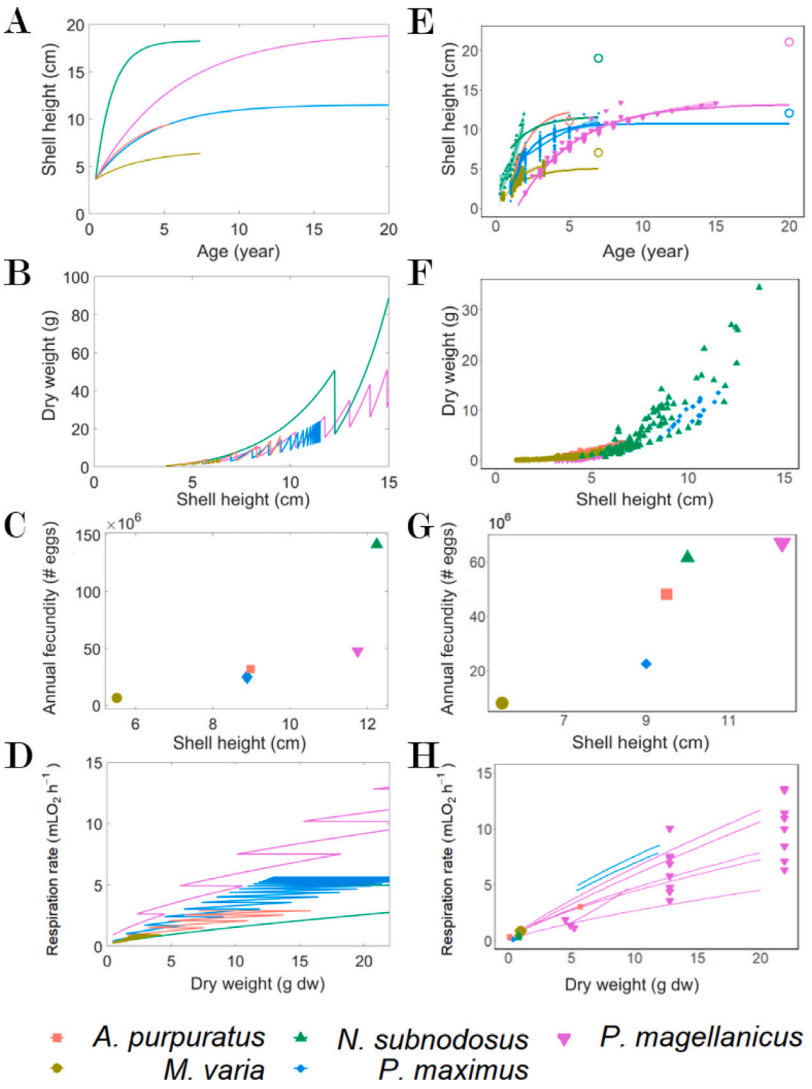

Fig. 3. Simulations with co-variation rules on maximum assimilation and maturity threshold at puberty (A–D) and observed variables from literature review, references in Section 2.1.2 (E–H). More specifically, for observed shell height at age (E), the curves represent von Bertalanffy growth curve and open circles correspond to ultimate shell heights at life span. Observed annual fecundity (G) corresponds to number of spawning times number of eggs per spawning times 2 for hermaphrodite species. For observed respiration rates (H), the curves represent allometric relationships with dry weight, converted at 20 °C for all species. Simulations were realised at typical temperature (8.5 °C for *P. magellanicus*, 25 °C for *N. subnodosus*, 12 °C for *P. maximus*, 15 °C for *A. purpuratus* and 13 °C for *M. varia*).

related to ultimate size (L_p = 3.6 ± 2 cm and a_p = 328 ± 190 d, cv = 60 % for both). *A. purpuratus* reaches puberty earlier and at a smaller size (2 cm at 62 days-old), while *N. subnodosus* is the largest and latest to mature, reaching puberty at a height of 6.6 cm and 590 days-old (Table 1). The values for *M. varia* are intermediate, and similar between *P. magellanicus* and *P. maximus*. Thus, the length at puberty generally correlates with ultimate length, except for *N. subnodosus*.

3.1.2. Shell height growth

In simulations using the null model (physical co-variation rules only), species with a higher maximum assimilation rate achieve a greater ultimate shell height. However, the observed ultimate shell heights can vary depending on the data source. Specifically, values derived from the von Bertalanffy growth equations (Supp. Table A.1) are larger than those obtained through literature review (Table 1). A comparison of simulations (Fig. 3A) with observed data (coloured points and curves on Fig. 3E) shows a similar ranking of species by ultimate shell height, except for *N. subnodosus*. At their typical temperature, *A. purpuratus* exhibits the highest growth rate according to the von Bertalanffy growth equation, followed by *P. maximus*, *N. subnodosus* and *M. varia*, which have comparable rates, and finally *P. magellanicus*.

3.1.3. Body condition

The simulations (Fig. 3B) suggest a cubic relationship between dry weight and shell height, with only minor variations among species. The species with the highest maximum size (purple curve) shows a greater weight at a given shell height, due to a higher maximum energy density. This pattern is also evident in the observed data for all five species (Fig. 3F). However, simulated weights are overestimated for *P. magellanicus* and *N. subnodosus*. The observed relationships between dry weight and shell height revealed significant differences in both intercepts and slopes among species (p-value < 2 10^{-16}). Slopes were found to be highest for *P. magellanicus* and *M. varia*, followed by *P. maximus*, *N. subnodosus* and *A. purpuratus* in descending order. Further details are provided in Supp. Tab. A.2.

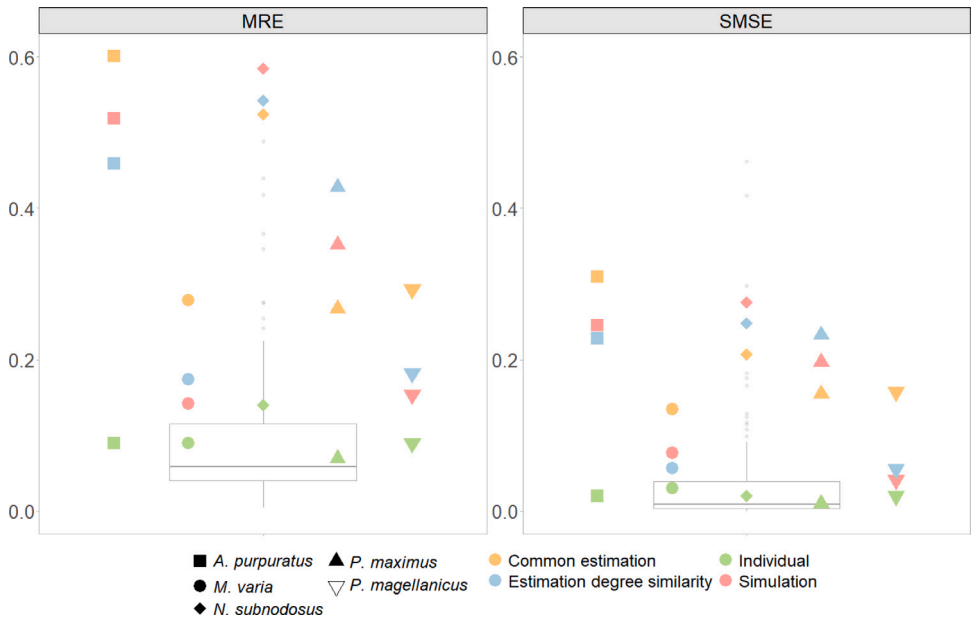

Fig. 4. Specific errors (Mean Relative Error, MRE and Symmetric Mean Squared Error, SMSE) between data and predictions for a 4-steps parameter estimation procedure: (i) individual estimation per species (green points), (ii) simulations based on *P. magellanicus* parameters applied to all species with physical co-variation rules for maturity at puberty (E_H^p) and maximum assimilation rate ($\{\dot{p}_{Am}\}$) (red points), (iii) common multi-species estimation considering all parameters equal between species except E_H^p and $\{\dot{p}_{Am}\}$ linked with physical co-variation rules (orange points) and (iv) multi-species estimation of $[\dot{p}_M]$ and $\dot{v}$ with a degree of similarity of 6 and physical co-variation rules on E_H^p and $\{\dot{p}_{Am}\}$ (blue points). Boxplot represents the distribution of MRE and SMSE for all parameter estimations of bivalves on Add-my-Pet portal (AmP, 2023).

3.1.4. Reproduction

The literature review (Table 2) shows that egg diameters are similar for *A. purpuratus*, *M. varia*, *P. maximus* and *P. magellanicus*, with a maximum variation of 10%. In contrast, the average egg diameter for *N. subnodosus* is 15 to 30% smaller than that of the other species. The number of oocytes spawned per event is 2 to 8 times higher for *P. magellanicus* compared to the other species. *A. purpuratus* spawns all year-round, surpassing the other species in event frequency. A strong allometric relationship exists between observed fecundity and shell height (Fig. 3G), with an adjusted R^2 of 0.86 and an exponent of 2.8. A similar pattern was observed in simulated fecundity relative to shell height, although the simulated relationship was less pronounced, particularly for *N. subnodosus*, which had notably higher simulated fecundity than observed.

3.1.5. Respiration rates

The power of the relationship between respiration rate and dry weight at the typical temperature appears similar between the simulations (Fig. 3D) and the observed data (Fig. 3H), with both exhibiting the same order of magnitude for respiration rate at a given dry weight. However, the observed data for *P. maximus* indicate higher respiration rates than those simulated based on the physical co-variation rules (blue lines in Fig. 3D and H). Depending on the dataset used, there exists a variability within the same species, such as *P. magellanicus* (magenta lines in Fig. 3H). Despite this, no clear relationship was identified in either the simulations or the observed data.

3.2. Parameter estimation

3.2.1. Individual estimation

From individual estimations, we derived a specific parameter set for each of the five species studied. For *N. subnodosus*, we estimated the first version of DEB parameters, achieving a MRE of 0.14 and a SMSE of 0.02 based on five uni-variate datasets and life-cycle traits. The MRE for individual estimations ranged from 0.07 for *P. maximus* to 0.144 for *N. subnodosus*, while the SMSE from 0.01 for *P. maximus* and 0.03 for *M. varia*. These error values fall within the range observed for all bivalves estimated in the AmP database, as shown in Fig. 4.

Individual parameter estimations revealed some variations among species. The coefficient of variation for the volume-species somatic maintenance ($[\dot{p}_M]$) was 77%, with values ranging from 18.4 for *N. subnodosus* to 153.8 for *A. purpuratus*. The allocation fraction to the somatic branch (κ) was consistent across most species, except for *P. magellanicus*, which had a lower value of 0.48 compared to 0.76 ± 0.07 (mean $\pm$ se) for the other four species. The energy conductance ($\dot{v}$) and the specific cost of structure ($[E_G]$) were similar across species. Parameter values from individual estimations are provided in Table 4, with the corresponding errors represented by the green points in Fig. 4.

3.2.2. Common multi-species estimation with co-variation pattern

Using common parameter estimation based on physical co-variation rules for maturity at puberty and maximum assimilation rate, we derived a single set of parameters applicable to all five species. The resulting overall MRE and SMSE were 0.48 and 0.31, respectively. With the common estimation (orange points in Fig. 4), the errors (MRE and SMSE) decreased for *N. subnodosus* and *P. maximus*, but were higher for *A. purpuratus*, *M. varia* and *P. magellanicus*, in comparison to the simulations based only on co-variation rules (red points in Fig. 4). For *N. subnodosus*, the zero-variate data were poorly predicted (Table 5), particularly for the length at puberty and ultimate length when compared to life cycle data (Table 1). Fig. 5 illustrates the predictions of length at age across different datasets for each species. The predictions were accurate for *M. varia* (Fig. 5B), *P. magellanicus* (Fig. 5C) and *P. maximus* (Fig. 5D) in one dataset. However, the growth predictions for *A. purpuratus* were less accurate, showing a very slow increase in size over time (Fig. 5A). Additional results, including predictions of weight at age and weight relative to length, are available in the supplementary materials. The weight-at-age relationships showed the least accurate predictions, with an overestimation for *N. subnodosus* and an underestimation for *A. purpuratus* and *M. varia*. For *A. purpuratus*, the trend of growth in weight was similar to that observed in the growth in size, with a very slow increase (Supp. Fig. B.1). The relationships between weight and shell height were accurately predicted for all three species: *M. varia*, *N. subnodosus* and *P. magellanicus* (Supp. Fig. B.2).

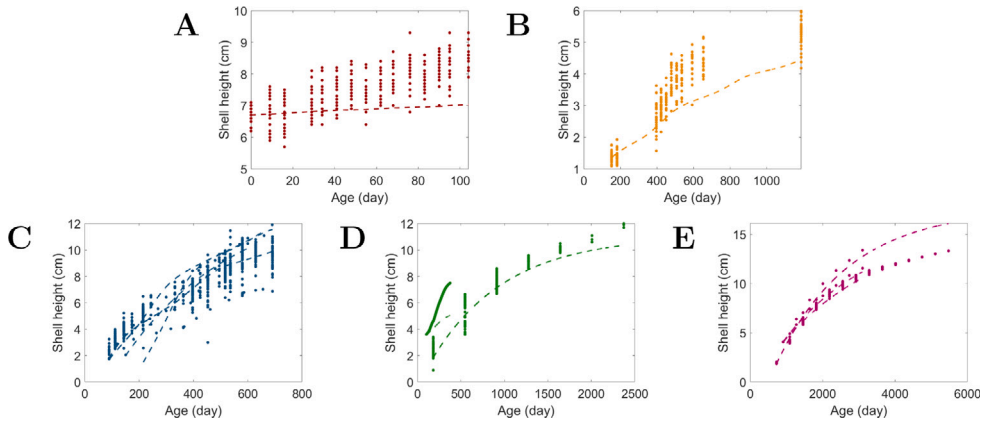

Fig. 5. Shell height at age, data (points) and predictions (dashed lines) using common multi-species parameter estimation with all parameters equal except the two defined by physical co-variation rules (maturity threshold at puberty and maximum assimilation rate), for *A. purpuratus* (A), *M. varia* (B), *N. subnodosus* (C), *P. maximus* (D) and *P. magellanicus* (E).

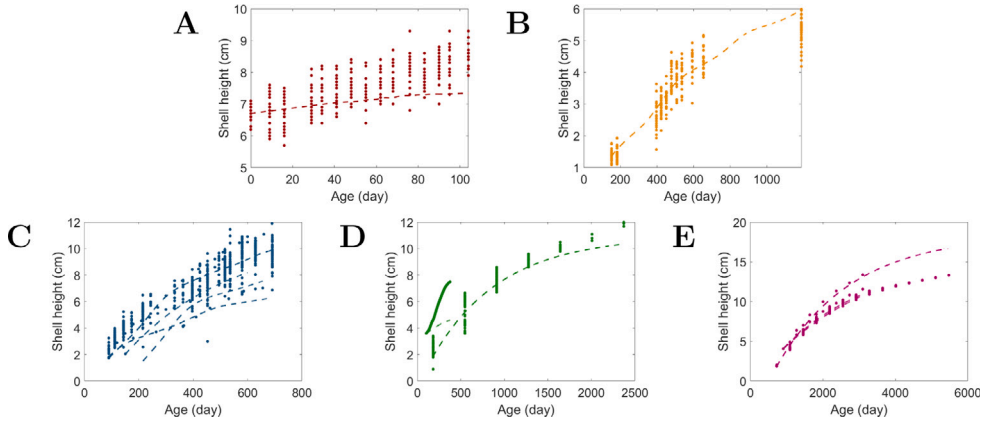

Fig. 6. Shell height at age, data (points) and predictions (dashed lines) using multi-species parameter estimation of energy conductance ($\dot{v}$) and somatic maintenance ($[\dot{p}_M]$) with a degree of similarity of 6. Initial parameters as *P. magellanicus* parameter values and physical co-variation rules on maturity threshold at puberty and maximum assimilation rate, for *A. purpuratus* (A), *M. varia* (B), *N. subnodosus* (C), *P. maximus* (D) and *P. magellanicus* (E).

3.2.3. Multispecies estimation with trait differences

The degree of similarity between species of somatic maintenance costs ($[\dot{p}_M]$) and energy mobilisation rate ($\dot{v}$) was incrementally increased from 0 (no constraint for similarities between parameters) to 6 (strong constraint for similarities between parameters) simultaneously. The predicted growth in shell height was accurate for four of the species: *M. varia*, *N. subnodosus*, *P. maximus* and *P. magellanicus* (Fig. 6B–E). However, the growth was still insufficient for *A. purpuratus* (Fig. 6A). This estimation enabled a more accurate prediction of growth in weight than the common estimation, except for *A. purpuratus*. The figures are available in the supplementary materials (Supp. Fig. C.1). The relationships between weight and shell height were accurately predicted for the three species: *M. varia*, *N. subnodosus* and *P. magellanicus* (Supp. Fig. C.2). Global errors for multi-species parameter estimation with degree of similarity of 6 were a MRE of 0.38 and a SMSE of 0.23. Errors per species were generally lower after parameter estimations than after simulations based on *P. magellanicus* parameters (blue points on Fig. 4).

Regarding parameter values, Fig. 7 shows the results for energy conductance and somatic maintenance obtained with multi-species parameter estimation with degrees of similarity ranging from 0 to 6. Each species is represented by six points corresponding to the six estimations with degree of similarity from 0 to 6 for $[\dot{p}_M]$ and $\dot{v}$. No trend is evident in the energy conductance values with respect to the "slow-to-fast depurator" gradient (Fig. 7A). However, an increasing trend is observed for somatic maintenance according to the "slow-to-fast depurator" gradient, with the exception of *P. maximus*. The final set of parameters for all species, derived from the estimation with the highest degree of similarity between species (6 as a degree of similarity for both $[\dot{p}_M]$ and $\dot{v}$) is provided in Table 4. The multispecies estimation with high similarity was the best predictions for *A. purpuratus* and *M. varia*, and the common estimation was the best for *P. maximus* and *N. subnodosus*, based on their overall SMSE (Table 4).

4. Discussion

In some pectinid species, such as *P. maximus*, toxic concentration of domoic acid (DA) for human consumption in body tissues can last for months following a harmful algal bloom. For other pectinids, such as *A. purpuratus*, DA seems to be absent from body tissues in the days following such bloom. In this study, in order to better understand the underlying mechanisms and robustly predict domoic acid depuration particularly in "slow" pectinid species, we investigated whether one or several physiological functions could be linked to the "slow" or "fast" trait of domoic acid depuration in pectinids. We performed our comparative approach within the Dynamic Energy Budget (DEB) theory framework, which led to three main contributions: *(i)* we successfully, after a thorough review of the existing literature, represented the full life cycle of five economically significant pectinid species and identified gaps and inconsistencies in the data available, *(ii)* we made advances in the application of the multi-species parameter estimation methodology

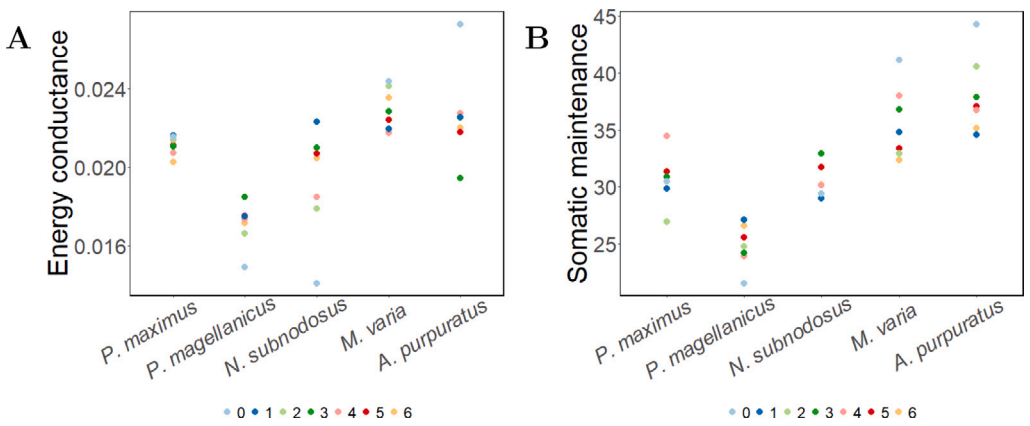

Fig. 7. Values of the two parameters estimated for the five species, (A) energy conductance $\dot{v}$ (cm d^{-1}) and (B) somatic maintenance $[\dot{p}_M]$ (J cm^{-3} d^{-1}). Results from parameter estimations with different values of degree of similarity (from 0 to 6, colour gradient) on somatic maintenance ($[\dot{p}_M]$) and energy conductance ($\dot{v}$) jointly.

for phylogenetically-related species and provided all the Matlab codes necessary to follow-up on this methodology, and *(iii)* we provided the model basis for the development of a toxico-kinetic module coupled to these pectinid life-cycle model that will allow to predict domoic acid depuration in pectinids as functions of the environmental conditions and the state of the individuals.

4.1. Life-trait comparison and interpretation

By synthesising a wide range of literature findings and previously unpublished data from the Tinduff hatchery, we created a comprehensive dataset that includes life cycle traits, growth parameters (such as shell height and weight), body condition indicators, reproductive characteristics, and respiration rates for the selected species. This dataset will be useful not only for future studies on the dynamics of DA depuration, but for all questions related to pectinid biodiversity.

Our findings only revealed small differences (coefficient of variation less than 50%) in the length and age at first feeding (birth) and metamorphosis in the data, suggesting shared developmental trajectories. We also found a correlation between the length at first reproduction (puberty) and ultimate shell height (Table 1). Our analysis identified a power-law relationship between reproductive effort (annual fecundity), and length at spawning event, that we were able to reproduce by considering a constant proportion of energy allocated to reproduction (*i.e.*, $1-\kappa$) across species. This relationship results in annual fecundity scaling with body size to the power of three. These patterns have already been studied within the framework of DEB theory for various taxa, including bivalves (Cardoso et al., 2006) and salmon (Pecquerie et al., 2011). Our results align closely with previous studies on bivalve comparison (Cardoso et al., 2006), wherein early life stages remained consistent traits among species despite variations in maximum body length. Unlike earlier multi-species DEB parameter studies (Lika et al., 2020; Guillaumot et al., 2020), our approach prioritised a common species and subsequently incorporated species-specific differences to better capture observed data patterns.

To comprehensively represent species within our framework, we integrated diverse data types, which carries the risk of introducing inconsistencies between datasets (Marques et al., 2019). Data inconsistency refers to the lack of correspondence between data from multiple datasets on physiological traits. In this study, this phenomenon was evident in the context of growth, where shell height measurements did not agree with the von Bertalanffy growth curves from other studies or with shell height measurements over time for *in situ* or experimental monitoring. These discrepancies may be due to environmental conditions, population differences or measurement errors. It is therefore of paramount importance to (i) document environmental conditions in which data were collected and (ii) detail the assumptions for the initial conditions of the state variables and the environmental conditions used to simulate the corresponding observables. It is only in the light of these (potentially lacking) information that model fit can be interpreted.

It is also important to document the assumptions made regarding stage transitions. DEB models require a single value for life cycle transitions, while, in reality, transitions such as metamorphosis or puberty can occur over several days or weeks. For puberty, the first reproductive event is often used as a reference point because it is the easiest to measure, but it only provides information about the end of the puberty transition. Differences between morphological and metabolic metamorphosis (*i.e.* metabolic acceleration) further illustrate the challenges of aligning model assumptions with "real world" observations.

In Fig. 2, we detailed the assumptions we made for this study, where settlement is assumed to correspond to the end of the metabolic acceleration period (DEB metamorphosis denoted "j"). However, discrepancies between data and model predictions for the juvenile period suggest that different model assumptions for the juvenile period, with limited consequences for the adult phase, could better fit the observations (see Section 4.3).

Our aim was to elucidate the main sources of life-history trait variation among the five pectinid studied species. Despite inherent discrepancies between observed data and model predictions, our analysis revealed consistent patterns in growth, body condition, and annual reproductive effort across species, using unified set of Dynamic Energy Budget (DEB) parameters, incorporating physical co-variation rules for maximum assimilation rate and maturity threshold at puberty. This underscores the significance of interspecies comparisons based on parameter values, facilitated by the AmP portal (AmP, 2023). This approach led us to make model assumptions that we discuss further in the following paragraphs.

Dry to wet weight ratio We reassessed the significance of the parameter associated to the dry to wet weight ratio, suggesting its dependence on the bivalve family under study. Specifically, the current proposed value in the AmP parameter estimation procedure (AmPtool, 2022) implies a higher water content than reported in the literature for these species around 80% (Aguirre-Velarde et al., 2019b; Carreño-León et al., 2023; DuPaul, 1970; Régnier-Brisson, 2024). This parameter was already adjusted for *P. maximus* in Lavaud et al. (2014) study. Adjusting this parameter (*i.e.*, density of structure, d_V) equal to the density of reserve (d_E) resulted in doubling the specific cost for the structure parameter ($[E_G]$) in order to take into account a lower water content.

Dataset-specific functional response Food availability is a prerequisite for each dataset, yet, in the majority of cases this information is absent from the source reports. In this study, we have chosen to initialise the functional responses at a value of 1 as a reference point for zero-variate data. In the estimation process, the values were permitted to fall below or above 1, with the objective of incorporating both quantity and

Table 4
Parameter values and errors (mean relative error (MRE) and symmetric mean squared error (SMSE)) for individual estimations ("Ind."), simulations with *Placopecten magellanicus* parameters and physical co-variation rules ("Simu."), common multi-species parameter estimation with all parameters equal except the ones implied in physical co-variation rules ("Comm.") and multi-species parameter estimation with differences on $\dot{v}$ and $[\dot{p}_M]$ ("Multi.", degree of similarity of 6).

Species	Method	Zoom factor	Max. spe. assim. rate	Energy conductance	Allocation fraction to soma	Vol-spe. som. maintenance	Spe. cost for structure	Maturity at birth	Mat. at metamorphosis	Mat. at puberty	Weibull ageing acceleration	Shape coeff.	MRE	SMSE
		z	$\{\dot{p}_{Am}\}$	$\dot{v}$	κ	$[\dot{p}_M]$	$[E_G]$	E_H^b	E_H^j	E_H^p	$\ddot{h}_a$	δ_M		
		–	J cm^{-2}d^{-1}	cm d^{-1}	–	J cm^{-3} d^{-1}	J cm^{-3}	J	J	J	d^{-2}	–	–	–
A. purpuratus	Ind.	0.69	125	0.019	0.85	153.8	5230	2.5 10^{-4}	0.032	361	5.5 10^{-8}	0.31	0.09	0.02
	Simu.	0.30	17	0.02	0.48	26.9	5181	2.4 10^{-3}	3.86	1815	2.8 10^{-9}	0.32	0.52	0.25
	Comm.	0.27	16	0.02	0.50	29.0	4192	2.8 10^{-3}	2.5	1893	2.9 10^{-9}	0.32	0.60	0.31
	Multi.	0.18	13	0.022	0.48	35.2	5181	2.4 10^{-3}	3.9	1815	3.0 10^{-9}	0.32	0.46	0.23
M. varia	Ind.	0.79	97	0.013	0.81	98.9	5296	2.3 10^{-4}	0.004	302	3.65 10^{-8}	0.28	0.09	0.03
	Simu.	0.35	20	0.02	0.48	26.9	5181	2.4 10^{-3}	3.86	468	2.8 10^{-9}	0.32	0.14	0.08
	Comm.	0.17	10	0.02	0.50	29.0	4192	2.8 10^{-3}	2.5	488	2.9 10^{-9}	0.32	0.28	0.14
	Multi.	0.11	8	0.024	0.48	32.4	5181	2.4 10^{-3}	3.9	468	3.0 10^{-9}	0.32	0.17	0.06
N. subnodosus	Ind.	1.28	29	0.013	0.82	18.41	5293	1.8 10^{-4}	0.030	22 980	1.76 10^{-8}	0.35	0.14	0.02
	Simu.	0.52	29	0.02	0.48	26.9	5181	2.4 10^{-3}	3.86	9354	2.8 10^{-9}	0.32	0.59	0.28
	Comm.	0.46	27	0.02	0.50	29.0	4192	2.8 10^{-3}	2.5	9757	2.9 10^{-9}	0.32	0.52	0.21
	Multi.	0.31	19	0.020	0.48	30.21	5181	2.4 10^{-3}	3.9	9354	3.0 10^{-9}	0.32	0.54	0.25
P. maximus	Ind.	0.98	75	0.014	0.82	62.63	5238	3.3 10^{-4}	0.017	3993	9.12 10^{-9}	0.31	0.07	0.01
	Simu.	0.33	19	0.02	0.48	26.9	5181	2.4 10^{-3}	3.86	2357	2.8 10^{-9}	0.32	0.35	0.20
	Comm.	0.29	17	0.02	0.50	29.0	4192	2.8 10^{-3}	2.5	2458	2.9 10^{-9}	0.32	0.27	0.16
	Multi.	0.19	13	0.020	0.48	31.37	5181	2.4 10^{-3}	3.9	2357	3.0 10^{-9}	0.32	0.43	0.23
P. magellanicus	Ind.	0.54	30	0.021	0.48	26.94	5181	2.4 10^{-3}	3.86	10 910	2.8 10^{-9}	0.33	0.09	0.02
	Simu.	0.54	30	0.02	0.48	26.9	5181	2.4 10^{-3}	3.86	10 910	2.8 10^{-9}	0.32	0.15	0.04
	Comm.	0.49	28	0.02	0.50	29.0	4192	2.8 10^{-3}	2.5	11 380	2.9 10^{-9}	0.32	0.29	0.16
	Multi.	0.32	18	0.017	0.48	26.6	5181	2.4 10^{-3}	3.9	10 910	3.0 10^{-9}	0.32	0.18	0.06

Table 5
Predictions of zero-variate data for each species based on individual estimations ("Ind."), simulations with *Placopecten magellanicus* parameters and physical co-variation rules ("Simu."), common multi-species parameter estimation with all parameters equal except the ones implied in physical co-variation rules ("Comm.") and multi-species parameter estimation with differences on $\dot{v}$ and $[\dot{p}_M]$ ("Multi.", degree of similarity of 6).

Species	Method	Age at birth	Age at metamorphosis	Age at puberty	Life span	Length at birth	Length at metam.	Length at puberty	Ultimate length
		a_b	a_j	a_p	a_m	L_b	L_j	L_p	L_i
		d	d	d	d	cm	cm	cm	cm
Argopecten purpuratus	Ind.	1.5	5.5	72	2073	0.0075	0.01	2.1	10.7
	Simu.	2.3	50	228	4084	0.0088	0.27	2.1	10.9
	Comm.	2.4	41	226	3891	0.011	0.26	2.2	8.9
	Multi.	2.1	41	189	3818	0.009	0.27	2.1	10.3
Mimachlamys varia	Ind.	1.6	6	199	2780	0.0083	0.05	1.9	7.0
	Simu.	2.2	78.5	294	3511	0.0088	0.27	1.3	6.9
	Comm.	2.2	64.9	285	3345	0.011	0.27	1.4	5.6
	Multi.	1.9	69.3	260	3210	0.009	0.27	1.3	6.5
Nodipecten subnodosus	Ind.	0.9	6.5	388	2166	0.0053	0.08	7.3	19.7
	Simu.	1.0	15.1	104	2550	0.0088	0.27	3.4	11.9
	Comm.	1.0	13	105	2429	0.011	0.26	3.7	15.4
	Multi.	1.0	14.5	98	2442	0.09	0.28	3.4	17.8
Pecten maximus	Ind.	2.0	6.9	386	6017	0.0080	0.08	4.3	11.8
	Simu.	2.3	46.0	193	5620	0.0088	0.27	1.4	11.9
	Comm.	2.3	38	190	5354	0.011	0.26	1.5	9.7
	Multi.	2.3	43	180	5400	0.009	0.27	1.4	11.2
Placopecten magellanicus	Ind.	2.7	41.8	332	7303	0.0105	0.12	3.7	19.2
	Simu.	2.8	41.9	333	7354	0.0088	0.1035	3.8	19.8
	Comm.	2.9	35.7	338	7006	0.011	0.10	4.1	16.3
	Multi.	3.3	46	361	7472	0.009	0.11	3.8	18.9

quality of food. In laboratory experiments, food is typically assumed to be unlimited, yet the quality may not be optimal for the individuals. Therefore, we believe that the scaled functional response may be lower for laboratory experiments than for *in situ* monitoring, when quality of the food is taken into account. Food quality is important to considered in DEB model, as already discussed for the New Zealand greenshell mussel (Ren, 2009) with the consideration of inorganic and organic food and modification of the functional response. The feeding on several food sources and the preferences between them have already been developed for *P. maximus* in Lavaud et al. (2014). Seasonal fluctuations of food quality and quantity in a region should also be considered to better reproduce the growth of individuals from field samples.

No trade-offs between growth and reproduction across species Following our data analysis, we assumed that the allocation to the soma fraction (κ) was constant across species, *i.e.* that differences in ultimate size were not a trade-off between growth and reproduction in large vs. small species. Our modelling choice to consider *P. magellanicus* as the reference species led us to consider a significantly lower value for κ (0.5) compared to the average soma fraction value of 0.88 for bivalves on AmP. It should be noted that many bivalve species have values exceeding 0.9, indicating a generally low reproductive effort among these species which could be debated given the uncertainty in annual reproductive energy investment data in multi-spawning species.

Overall, we provided the first DEB parameter set for *N. subnodosus* and proposed new parameter sets for the other four species, tailored for the region of interest, *i.e.* datasets outside of the spatial distribution of interests were not considered in our study. Each of the five species studied however has its own value for future single-species studies based on our DEB parameter values. We achieved to decrease the errors between predictions and observations (mean relative error, MRE and symmetric mean squared error, SMSE) for *A. purpuratus*, *P. magellanicus* and *M. varia* compared to previous parameter sets (AmP, 2023; Régnier-Brisson, 2024), and for *P. maximus*, we provided a new parameter set focused on the Bay of Brest.

4.2. Evidence for a "slow-to-fast-depurator" range

Maximum assimilation rate We investigated specific DEB parameters thought to influence differences in toxin retention across species. As expected, larger species exhibited higher maximum assimilation rates, following the physical co-variation rules. However, contrary to the expectations based on the "slow-to-fast-depurator" range, the Bay of Brest *P. maximus*, which should typically exhibit the highest toxin assimilation, did not fit this pattern. These findings suggest that a careful attention should be given to food-specific assimilation rates. Selective ingestion rates have been observed in other species, such as *Crassostrea virginica* (Mafra Jr. et al., 2009) and in laboratory comparisons between *C. gigas* (now *Magallana gigas*) and *P. maximus* (Sauvey et al., 2021). Unfortunately, we lacked filtration rate data for all species, which could have clarified potential differences in toxin assimilation mechanisms among these species.

Mobilisation rate We initially hypothesised that species with higher toxin depuration rates might exhibit higher energy conductance, which controls reserve mobilisation. A higher energy conductance typically leads to shorter development times, faster growth rates, and lower maximum reserve density (Lika et al., 2011). However, during our parameter estimation procedure, we only found minor differences in energy conductance values even when we released the similarity degree between species for this parameter. No clear pattern between energy conductance and "slow-to-fast" gradient could be seen in our results. Regardless of the degree of similarity applied to this parameter, *P. magellanicus* seems to have the lowest value of energy conductance, which corroborates the hypothesis of that it is a slow depurator.

Somatic maintenance Our second hypothesis was that volume-specific somatic maintenance costs ($[\dot{p}_M]$) would be higher for species with higher depuration rates. In DEB theory, these costs represent the maintenance of concentration gradients at the membrane level and protein turnover (Kooijman, 2010). Changes in maintenance costs can reflect impacts on immune response or detoxification processes, as demonstrated in oysters affected by paralytic shellfish toxin Pousse et al. (2019). We hypothesised that differences in these processes between species could explain variations in contamination levels and decontamination rates. For example, *P. maximus* was found to have a higher quantity of autophagosomes in its tissues, particularly in the digestive gland, compared to other species (García-Corona et al., 2022). While the physiological effects of domoic acid and *Pseudo-nitzschia* spp. on bivalves are not fully understood, variations in cellular processes, such as immune response and membrane transport, may contribute to differences in somatic maintenance costs. Based on this hypothesis, *A. purpuratus*, *M. varia* and *N. subnodosus* were expected to have higher maintenance costs compared to *P. magellanicus* and *P. maximus*. This pattern was observed in our results, except for *P. maximus*. Notably, the highest value for *A. purpuratus* was expected considering its high metabolic performance and relatively short ultimate size, as discussed in previous studies (Aguirre-Velarde et al., 2019a). However, our results suggest variability of this trait among species, indicating that this hypothesis requires further investigation. We also found that $[\dot{p}_M]$ values were highly sensitive to initial parameter values and to the weighting applied to emphasise different datasets. Additionally, $[\dot{p}_M]$ values varied significantly among species in individual DEB parameter estimations, ranging from 18 J cm^{-3} d^{-1} for *N. subnodosus* to 150 J cm^{-3} d^{-1} for *A. purpuratus*. Previous studies have suggested that $[\dot{p}_M]$ should be similar among related species at similar temperature near their optimal conditions (van der Veer et al., 2006). However, this highlights the need for further research to determine whether $[\dot{p}_M]$ should be constrained to a small range among closely related species or if greater variability is appropriate. Establishing a range of values for closely related species could clarify whether this parameter should indeed be tightly constrained. Short-term experiments of starvation could be realised to precise the variations of the somatic maintenance costs ($[\dot{p}_M]$), which also depend on the mobilisation rate. This approach could provide insights into differences in toxin kinetics based on this physiological trait.

In this study, we focused on delineating physiological similarities and differences among pectinid species, considering their phylogenetic distance. Our goal was to determine physiological processes potentially linked to toxin kinetics. However, the four parameters investigated: maximum assimilation rate, maturity threshold at puberty, somatic maintenance and energy conductance ($\{\dot{p}_{Am}\}$, $[E_H^p]$, $[\dot{p}_M]$, and $\dot{v}$, respectively), were insufficient to fully capture the observed data. It is likely that differences in toxin kinetics stem from a combination of multiple parameters and associated life traits. Species-specific responses to toxins may also result from acclimation or adaptation to regional environmental conditions, where certain species may have developed enhanced toxin depuration capacities. For example, regular exposure of *Mya arenaria* populations to the paralytic shellfish toxin has led to genetic adaptations (Bricelj et al., 2005), enabling these populations to accumulate higher levels of toxins than less exposed populations. Environmental plasticity is recognised to significantly influence both intra-species (MacDonald and Thompson, 1988; Lubet et al., 1995) and inter-species variations, especially concerning differences in life traits (Alejandrino et al., 2011). Comparing species has enabled us to refine our assumptions and adding more species to the comparison would allow us to narrow them down even further. However, providing managers with useful tools will still require site-specific studies.

4.3. Improvement and potential of the approach

Continuing to compare pectinid species offers potential for elucidating differences in life traits, particularly concerning domoic acid retention and depuration. Expanding the scope to include additional species would provide a more robust assessment of whether a unified

set of parameters with physical co-variation rules remains applicable across diverse species. Although no link between parameter sets and phylogenetic was found in this study, further studies should include species that are distributed along the phylogenetic tree and inhabiting habitats with contrasting environmental conditions. For example, adding the Queen scallop, *Aequipecten opercularis* (Linnaeus, 1758), one of the most distantly related species within the Pectinidae family (Fig. 1), could reinforce observed patterns in life traits related to toxin kinetics, despite limited data on its toxin depuration rate (Kvrgić et al., 2022; García-Corona et al., 2024).

However, limitations in the multi-species parameter estimation process were observed when four species were incorporated. The method appeared overly restrictive, with parameter values remaining close to their initial values across multiple runs, suggesting an incomplete exploration of the parameter space. Therefore, while continued collection of life-trait data is essential, refinement of the parameter estimation procedure, especially for multi-species analyses, is necessary.

Our parameter estimation focused exclusively on adult stage data, including life cycle, growth, body condition, and reproduction data due to limited data on early life stages and the challenges in predicting both early and adult stages simultaneously. Although this approach aligns with our primary objective concerning toxin kinetics in adults, it has also highlighted new hypotheses regarding metamorphosis and the definition of larval and juvenile stages for pectinid species within the DEB model framework. Smaller larvae from hatchery or experimental settings have a better chance of reaching adulthood compared to those in natural environments, potentially leading to inconsistencies when combining data from both populations. Thus, using multiple population types (*i.e.*, hatchery larvae and field juveniles and adults) could complicate parameter estimation, and applying dataset-specific weighting for larvae may prove useful. The lack of a satisfactory fit between the model and the larval data led us to consider that physiological and morphological metamorphosis may not occur simultaneously. The model's metamorphosis threshold generally aligns with physiological changes, while observed variables often reflect physical changes, such as settlement. In this study, using the "abj" model, where metabolic acceleration of assimilation and mobilisation occurs from birth (first feeding) to metamorphosis, model predictions indicated a greater length and younger age at metamorphosis compared to observed data. To improve these predictions, metabolic acceleration should occur over a shorter period. Implementing the alternative "asj" model (Augustine et al., 2014), which represents acceleration ("a") between settlement ("s") and juvenile threshold ("j"), could offer more insights for early life stages. This model has been used for oyster species (Stechele et al., 2022) and could enhance estimates for pectinids.

Considering the life cycle of pectinids (Fig. 2A), we propose that metabolic acceleration may occur between settlement and when the individual reaches the adult form, corresponding to the "spat" stage in the literature. With these modifications, the DEB life cycle (Fig. 2B) would include five life stages: embryo, larva, post-larva, spat, adult, along with four transitions: birth, settlement, metamorphosis and puberty. The spat transition, commonly mentioned in scallop cultivation protocols, refers to when individuals are transferred to seawater for growth. Data on length at the spat transition has been compiled in Table 1, for further analyses using the "asj" model.

Reproductive effort significantly influences the energy budget of pectinids, and other bivalves, especially during certain seasons. Before spawning, gonad wet weight can account for up to 20% in *M. varia* (Régnier-Brisson, 2024) and up to 40% in *N. subnodosus* of the tissue wet weight (Maeda-Martínez and Lodeiros-Seijo, 2011). However, tracking individual annual reproductive effort is challenging and often requires proxies derived from population-level data, which are method-dependent and may not accurately reflect individual values. Thus, the calculating of reproductive effort relies heavily on the selected data and underlying assumptions, as demonstrated in this study during the literature review and parameter estimation. The studied species exhibit three reproductive strategies: gonochoric, successive hermaphrodite, and simultaneous hermaphrodite, each requiring specific considerations in reproductive effort calculations. For simultaneous hermaphrodites, like *M. varia*, doubling fecundity, or halving the reproductive efficiency (κ_R), may be necessary to avoid underestimating annual reproductive effort. Specific studies, such as HermaDEB for successive hermaphrodites (Louati et al., 2020), have been developed to incorporate reproductive types into DEB models, offering potential applications for species like *M. varia*. Further investigation, including determining gonad weight and gamete counts for both female and male reproductive material, is crucial for refining hypotheses about simultaneous hermaphrodite species.

Our study proposes a framework that could enhance data collection within the context of DEB theory, especially for species comparison, as emphasised by van der Veer et al. (2006). Our review revealed disparities in the attention given to different species and data types over time. This approach underscores the need for more comprehensive datasets and focused experimental efforts to better understand physiological variations among species. Specifically, providing explicit gonad weight alongside tissue weight, and detailing information on reproductive seasons, can offer valuable insights into the energy budget composition, particularly the contribution of reproduction. Understanding this contribution is essential for meaningful species comparisons within a bioenergetic conceptual framework. When data are limited, allometric relationships can provide an averaged individual information but may overlook inter-individual variability. It is important to recognise the limitations of extrapolating beyond the available data range. However, as noted by Cardoso et al. (2006), patterns identified through DEB theory can provide insights into unexplored areas, compensating for data gaps. Facilitating access to comprehensive datasets, covering several years (in our study, from 1980 to 2024), and presenting them in tabular formats alongside figures and/or data papers, can greatly aid literature reviews and enhance the completeness of species life trait documentation. This study highlights the importance of maintaining and sharing long-term data to foster a more robust understanding of species physiology.

5. Conclusion

This study offers new insights into the physiological differences across five pectinid species, by obtaining DEB parameters for a new species in the AmP collection: *N. subnodosus*, and proposing new estimations for the four other species: *P. maximus*, *P. magellanicus*, *M. varia* and *A. purpuratus*. Using the DEB theory framework, we demonstrated the feasibility of representing these species with a unified parameter set that includes physical co-variation rules for assimilation and maturity at puberty. Introducing life-trait differences incrementally allowed us to better match observations and identify significant variations in traits. Further investigations into toxin retention and depuration processes are warranted based on these findings. Integrating DEB models with individual bioenergetics and a toxin kinetic module, as applied to oysters exposed to *Alexandrium minutum* in Pousse et al. (2019), holds promise. Additionally, this comparative methodology has potential for phylogenetic studies, DEB parameters are used to construct life trees based on species distances (Kooijman et al., 2021). Such an approach may help to extrapolate toxin dynamics for species lacking direct data, withing the "slow-to-fast-depurator" range.

CRediT authorship contribution statement

Eline Le Moan: Writing – review & editing, Writing – original draft, Visualization, Software, Methodology, Investigation, Formal analysis, Data curation, Conceptualization. **Laure Pecquerie:** Writing – review & editing, Validation, Software, Methodology, Data curation, Conceptualization. **Laure Régnier-Brisson:** Resources, Formal analysis, Data

curation. **Hélène Hégaret:** Writing – review & editing, Supervision, Resources, Project administration, Funding acquisition, Conceptualization. **Paulo F. Lagos:** Writing – review & editing, Formal analysis. **Léo Heyer:** Data curation. **Salvador Emilio Lluch-Cota:** Supervision, Resources, Investigation. **Fred Jean:** Supervision, Funding acquisition, Conceptualization. **Jonathan Flye-Sainte-Marie:** Writing – review & editing, Validation, Supervision, Conceptualization.

Declaration of competing interest

The authors declare that they have no known competing financial interests or personal relationships that could have appeared to influence the work reported in this paper.

Acknowledgements

The authors are grateful to the Tinduff hatchery for providing data on both *Pecten maximus* and *Mimachlamys varia* and Ilie Racotta and the CONACYT CF2019-78911 project for sharing expert knowledge and data on *Nodipecten subnodosus*. We would like to thank Bas Kooijman for his meticulous correction of the estimation codes, as well as to all those who contributed to the codes used on AmP for certain species. This work received financial support from the research project "MaSCoET" (Maintien du stock de coquillages en lien avec la problématique des efflorescences toxiques) financed by France Filière Pêche and Brest Métropole. Eline Le Moan was recipient of a doctorate fellowship financed by France Filière Pêche and Région Bretagne. Paulo F. Lagos received financial support from ISblue project, Interdisciplinary graduate school for the blue planet (ANR-17-EURE-0015) and co-funded by a grant from the French government under the program "Investissements d'Avenir" embedded in France 2030.

Appendix A. Supplementary data

Supplementary material related to this article can be found online at https://doi.org/10.1016/j.ecolmodel.2024.110921.

Data availability

All data and codes are available at Github repository cited in the manuscript.

References

Abasolo-Pacheco, F., Mazón-Suástegui, J.M., Saucedo, P.E., 2009. Response and condition of larvae of the scallops *Nodipecten subnodosus* and *Argopecten ventricosus* reared at the hatchery with different seawater sources. Aquaculture 296 (3), 255–262. http://dx.doi.org/10.1016/j.aquaculture.2009.08.028, URL https://www.sciencedirect.com/science/article/pii/S0044848609007418.

Aguirre-Velarde, A., 2016. Bioenergetics of the Peruvian scallops (*Argopecten purpuratus*) in an environmental context limiting oxygen (Ph.D. thesis). Université de Bretagne occidentale - Brest, URL https://tel.archives-ouvertes.fr/tel-01542077.

Aguirre-Velarde, A., Jean, F., Thouzeau, G., Flye-Sainte-Marie, J., 2016. Effects of progressive hypoxia on oxygen uptake in juveniles of the Peruvian scallop, *Argopecten purpuratus* (Lamarck, 1819). Aquaculture 451, 385–389. http://dx.doi.org/10.1016/j.aquaculture.2015.07.030, URL https://www.sciencedirect.com/science/article/pii/S0044848615301125.

Aguirre-Velarde, A., Pecquerie, L., Jean, F., Thouzeau, G., Flye-Sainte-Marie, J., 2019a. Predicting the energy budget of the scallop *Argopecten purpuratus* in an oxygen–limiting environment. J. Sea Res. 143, 254–261. http://dx.doi.org/10.1016/j.seares.2018.09.011, URL https://www.sciencedirect.com/science/article/pii/S1385110118300327.

Aguirre-Velarde, A., Thouzeau, G., Jean, F., Mendo, J., Cueto-Vega, R., Kawazo-Delgado, M., Vásquez-Spencer, J., Herrera-Sanchez, D., Vega-Espinoza, A., Flye-Sainte-Marie, J., 2019b. Chronic and severe hypoxic conditions in Paracas Bay, Pisco, Peru: Consequences on scallop growth, reproduction, and survival. Aquaculture 512, 734259. http://dx.doi.org/10.1016/j.aquaculture.2019.734259, URL https://www.sciencedirect.com/science/article/pii/S0044848619304831.

Ahyong, S., Boyko, C., Bailly, N., Bernot, J., Bieler, R., Brandão, S., Daly, M., De Grave, S., Gofas, S., Hernandez, F., Hughes, L., Neubauer, T., Paulay, G., Boydens, B., Decock, W., Dekeyzer, S., Vandepitte, L., Vanhoorne, B., Adlard, R., Agatha, S., Ahn, K., Akkari, N., Alvarez, B., Alves, W., Amler, M., Amorim, V., Anderberg, A., Andrés-Sánchez, S., Ang, Y., Antić, D., Antonietto, L., Arango, C., Artois, T., Atkinson, S., Auffenberg, K., Baldwin, B., Bank, R., Barber, A., Barbosa, J., Bartsch, I., Bellan-Santini, D., Bergh, N., Berta, A., Bezerra, T., Blanco, S., Blasco-Costa, I., Blazewicz, M., Bł ędzki, L., Bock, P., Bonifacino, M., Böttger-Schnack, R., Bouchet, P., Boury-Esnault, N., Bouzan, R., Boxshall, G., Bray, R., Brito Seixas, A., Bruce, N., Bruneau, A., Budaeva, N., Bueno-Villegas, J., Cairns, S., Calvo Casas, J., Cárdenas, P., Carstens, E., Cedhagen, T., Chan, B., Chan, T., Cheng, L., Choong, H., Christenhusz, M., Churchill, M., Collins, A., Collins, G., Collins, K., Consorti, L., Copilaş-Ciocianu, D., Corbari, L., Cordeiro, R., Costa, V., Costa Corgosinho, P., Coste, M., Costello, M., Crandall, K., Cremonte, F., Cribb, T., Cutmore, S., Dahdouh-Guebas, F., Daneliya, M., Dauvin, J., Davie, P., De Broyer, C., de Lima Ferreira, P., de Mazancourt, V., de Sá, H., de Voogd, N., Decker, P., Defaye, D., Dekker, H., d'Hondt, J., Di Capua, I., Dippenaar, S., Dohrmann, M., Dolan, J., Domning, D., Downey, R., Dreyer, N., Eisendle, U., Eitel, M., Enghoff, H., Epler, J., Espindola, B., Esquete Garrote, P., Evenhuis, N., Ewers-Saucedo, C., Faber, M., Ferreira, M., Figueroa, D., Fišer, C., Fordyce, E., Foster, W., Fransen, C., Freire, S., Fujimoto, S., Furuya, H., Galbany-Casals, M., Gale, A., Galea, H., Gao, T., Garic, R., Garnett, S., Gaviria-Melo, S., Gerken, S., Gibson, D., Gibson, R., Gil, J., Gittenberger, A., Glasby, C., Glenner, H., Glover, A., Gómez-Noguera, S., Gondim, A., Gonzalez, B., González-Solís, D., Goodwin, C., Gostel, M., Grabowski, M., Gravili, C., Grossi, M., Guerra-García, J., Guerrero, J., Guidetti, R., Guiry, M., Gutierrez, D., Hadfield, K., Hajdu, E., Halanych, K., Hallermann, J., Hayward, B., Hegna, T., Heiden, G., Hendrycks, E., Herbert, D., Herrera Bachiller, A., Hodda, M., Hø eg, J., Hoeksema, B., Holovachov, O., Hooge, M., Hooper, J., Horton, T., Houart, R., Huys, R., Hyžný, M., Iniesta, L., Iseto, T., Iwataki, M., Janssen, R., Jaume, D., Jazdzewski, K., Jersabek, C., Jóźwiak, P., Kabat, A., Kakui, K., Kantor, Y., Karanovic, I., Karapunar, B., Karthick, B., Kathirithamby, J., Katinas, L., Kim, Y., King, R., Kirk, P., Klautau, M., Kociolek, J., Köhler, F., Konowalik, K., Kotov, A., Kovács, Z., Kremenetskaia, A., Kristensen, R., Kroh, A., Kulikovskiy, M., Kullander, S., Kupriyanova, E., Lamaro, A., Lambert, G., Lazarus, D., Le Coze, F., Le Roux, M., LeCroy, S., Leduc, D., Lefkowitz, E., Lemaitre, R., Lichter-Marck, I., Lim, S., Lindsay, D., Liu, Y., Loeuille, B., Lörz, A., Ludwig, T., Lundholm, N., Macpherson, E., Mah, C., Mamos, T., Manconi, R., Mapstone, G., Marek, P., Marshall, B., Marshall, D., Martin, P., McFadden, C., McInnes, S., McKenzie, R., Means, J., Mees, J., Mejía-Madrid, H., Meland, K., Merrin, K., Miller, J., Mills, C., Moestrup, O., Mokievsky, V., Molodtsova, T., Monniot, F., Mooi, R., Morandini, A., Moreira da Rocha, R., Morrow, C., Mortelmans, J., Muñoz Gallego, A., Musco, L., Nascimento, J., Nesom, G., Neubert, E., Neuhaus, B., Ng, P., Nguyen, A., Nielsen, C., Nielsen, S., Nishikawa, T., Norenburg, J., O'Hara, T., Opresko, D., Osawa, M., Osigus, H., Ota, Y., Páll-Gergely, B., Panero, J., Pasini, E., Patterson, D., Pedram, M., Pelser, P., Peña Santiago, R., Pereira, J., Perez-Losada, M., Petrescu, I., Pfingstl, T., Piasecki, W., Pica, D., Picton, B., Pignatti, J., Pilger, J., Pinheiro, U., Pisera, A., Poatskievick Pierezan, B., Polhemus, D., Poore, G., Potapova, M., Praxedes, R., P° uža, V., Read, G., Reich, M., Reimer, J., Reip, H., Resende Bueno, V., Reuscher, M., Reynolds, J., Richling, I., Rimet, F., Ríos, P., Rius, M., Rodríguez, E., Rogers, D., Roque, N., Rosenberg, G., Rützler, K., Saavedra, M., Sabbe, K., Sabroux, R., Saiz-Salinas, J., Sala, S., Santagata, S., Santos, S., Santos, S., Sar, E., Saucède, T., Schärer, L., Schierwater, B., Schilling, E., Schmidt-Lebuhn, A., Schmidt-Rhaesa, A., Schneider, S., Schönberg, C., Schuchert, P., Schweitzer, C., Semple, J., Senna, A., Sennikov, A., Serejo, C., Shaik, S., Shamsi, S., Sharma, J., Shear, W., Shenkar, N., Short, M., Sicinski, J., Sierwald, P., Silva, D., Silva, E., Simmons, E., Sinniger, F., Sinou, C., Sivell, D., Sket, B., Smit, H., Smit, N., Smol, N., Sø rensen, M., Souza-Filho, J., Spelda, J., Sterrer, W., Stoev, P., Stöhr, S., Suárez-Morales, E., Susanna, A., Suttle, C., Swalla, B., Taiti, S., Tanaka, M., Tandberg, A., Tang, D., Tasker, M., Taylor, J., Taylor, J., Taylor, K., Tchesunov, A., Temereva, E., ten Hove, H., ter Poorten, J., Thomas, J., Thuesen, E., Thurston, M., Thuy, B., Timi, J., Todaro, A., Todd, J., Turon, X., Uetz, P., Urbatsch, L., Uribe-Palomino, J., Urtubey, E., Utevsky, S., Vacelet, J., Vachard, D., Vader, W., Väinölä, R., Valls Domedel, G., Van de Vijver, B., van der Meij, S., van Haaren, T., van Soest, R., Vanreusel, A., Venekey, V., Verhoeff, T., Vinarski, M., Vonk, R., Vos, C., Vouilloud, A., Walker-Smith, G., Walter, T., Watling, L., Wayland, M., Wesener, T., Wetzel, C., Whipps, C., White, K., Wieneke, U., Williams, D., Williams, G., Wilson, R., Witkowski, J., Wyatt, N., Xavier, J., Xu, K., Zanol, J., Zeidler, W., Zhao, Z., Zullini, A., 2023. World Register of Marine Species (WoRMS). WoRMS Editorial Board, URL https://www.marinespecies.org.

Alejandrino, A., Puslednik, L., Serb, J.M., 2011. Convergent and parallel evolution in life habit of the scallops (Bivalvia: Pectinidae). BMC Evol. Biol. 11 (1), 164. http://dx.doi.org/10.1186/1471-2148-11-164, URL http://dx.doi.org/10.1186/1471-2148-11-164.

Álvarez, O.A., Rengel, J., Araya, M., Álvarez, F., Pino, R., Uribe, E., Díaz, P.A., Rossignoli, A.E., López-Rivera, A., Blanco, J., 2020. Rapid domoic acid depuration in the scallop *Argopecten purpuratus* and its transfer from the digestive gland to other organs. Toxins 12 (11), 698. http://dx.doi.org/10.3390/toxins12110698, URL https://www.mdpi.com/2072-6651/12/11/698. Number: 11 Publisher: Multidisciplinary Digital Publishing Institute.

AmP, 2023. Add-my-Pet collection, add-my-pet collection, online database of deb parameters, implied properties and referenced underlying data. URL http://www.bio.vu.nl/thb/deb/deblab/add_my_pet/.

AmPtool, 2022. AmP collection. URL https://github.com/add-my-pet/AmPtool. original-date: 2019-12-21T15:53:41Z.

Angel-Dapa, M.A., Arellano-Martínez, M., Ceballos-Vázquez, B.P., Acosta-Salmón, H., Saucedo, P.E., 2015. Comparative analysis of the reproductive strategy of lion's paw scallop *Nodipecten subnodosus* in Baja California Sur, Mexico. Latin Am. J. Aquatic Res 43 (3), 616–620. http://dx.doi.org/10.3856/vol43-issue3-fulltext-25, URL https://www.lajar.cl/index.php/rlajar/article/view/vol43-issue3-fulltext-25. Number: 3.

Arellano-Martínez, M., Ceballos-Vázquez, B.P., Ruíz-Verdugo, C., Pérez de León, E., Cervantes-Duarte, R., Domínguez-Valdéz, P.M., 2011. Growth and reproduction of the lion's paw scallop *Nodipecten subnodosus*in a suspended culture system at Guerrero Negro lagoon, Baja California Sur, Mexico. Aquacult. Res. 42 (4), 571–582. http://dx.doi.org/10.1111/j.1365-2109.2010.02652.x, URL https://onlinelibrary.wiley.com/doi/abs/10.1111/j.1365-2109.2010.02652.x.

Artigaud, S., Lacroix, C., Pichereau, V., Flye-Sainte-Marie, J., 2014. Respiratory response to combined heat and hypoxia in the marine bivalves *Pecten maximus* and *Mytilus spp.*. Comparat. Biochem. Physiol. A: Molecul. Integr. Physiol 175, 135–140. http://dx.doi.org/10.1016/j.cbpa.2014.06.005, URL https://www.sciencedirect.com/science/article/pii/S1095643314001184.

Augustine, S., Jaspers, C., Kooijman, S.A.L.M., Carlotti, F., Poggiale, J.-C., Freitas, V., Veer, H.v.d., Walraven, L.v., 2014. Mechanisms behind the metabolic flexibility of an invasive comb jelly. J. Sea Res. 94, 156–165.

Avendaño, M., 2001. Anormalidades en larvas de *Argopecten purpuratus* (Lamarck, 1819). Estud. Oceanol. 20, 33–42.

Blanco, J., Acosta, C., Mariño, C., Muñiz, S., Martín, H., Moroño, A., Correa, J., Arévalo, F., Salgado, C., 2006. Depuration of domoic acid from different body compartments of the king scallop *Pecten maximus* grown in raft culture and natural bed. 19, http://dx.doi.org/10.1051/alr:2006026, http://dx.doi.org/10.1051/alr:2006026.

Blanco, J., Acosta, C., Bermúdez de la Puente, M., Salgado, C., 2002. Depuration and anatomical distribution of the amnesic shellfish poisoning (ASP) toxin domoic acid in the king scallop *Pecten maximus*. Aquat. Toxicol. 60 (1–2), 111–121. http://dx.doi.org/10.1016/S0166-445X(01)00274-0, URL https://linkinghub.elsevier.com/retrieve/pii/S0166445X01002740.

Blanco, J., Mauríz, A., Alvarez, G., 2020. Distribution of domoic acid in the digestive gland of the King Scallop *Pecten maximus*. Toxins 12, http://dx.doi.org/10.3390/toxins12060371.

Bodiguel, X., Maury, O., Mellon-Duval, C., Roupsard, F., Le Guellec, A.-M., Loizeau, V., 2009. A dynamic and mechanistic model of PCB bioaccumulation in the European hake (*Merluccius merluccius*). J. Sea Res. 62 (2), 124–134. http://dx.doi.org/10.1016/j.seares.2009.02.006, URL https://www.sciencedirect.com/science/article/pii/S1385110109000264. Metabolic organization: 30 years of DEB applications and developments.

von Brand, E., Abarca, A., Merino, G.E., Stotz, W., 2016. Chapter 26 - Scallop Fishery and Aquaculture in Chile: A history of developments and declines. In: Shumway, S.E., Parsons, G.J. (Eds.), Developments in Aquaculture and Fisheries Science. In: Scallops, vol. 40, Elsevier, pp. 1047–1072. http://dx.doi.org/10.1016/B978-0-444-62710-0.00026-2, URL https://www.sciencedirect.com/science/article/pii/B9780444627100000262.

Bricelj, V.M., Connell, L., Konoki, K., MacQuarrie, S.P., Scheuer, T., Catterall, W.A., Trainer, V.L., 2005. Sodium channel mutation leading to saxitoxin resistance in clams increases risk of PSP. Nature 434 (7034), 763–767. http://dx.doi.org/10.1038/nature03415, URL https://www.nature.com/articles/nature03415.

Buestel, D., Laurec, A., 1975. Croissance de la coquille saint-jacques (*Pecten maximus* L.) en rade de Brest et en baie de Saint-Brieuc. Haliotis 5, 279–283, URL https://archimer.ifremer.fr/doc/00000/5093/. Publisher: Société Française de Malacologie.

Cardoso, J.F.M.F., van der Veer, H.W., Kooijman, S.A.L.M., 2006. Body-size scaling relationships in bivalve species: A comparison of field data with predictions by the dynamic energy budget (DEB) theory. J. Sea Res. 56 (2), 125–139. http://dx.doi.org/10.1016/j.seares.2006.05.001, URL https://www.sciencedirect.com/science/article/pii/S1385110106000670. Dynamic Energy Budgets in Bivalves.

Carnegie, R., 1994. Size-specific fecundity of the sea scallop, *Placopecten magellanicus*, during one spawning period in the mid-Atlantic resource area (Ph.D. thesis). College of William and Mary - Virginia Institute of Marine Science, URLhttps://doi.org/10.25773/v5-4xkj-k930. Publisher: College of William and Mary - Virginia Institute of Marine Science.

Carreño-León, D., Vázquez-Sánchez, R.I., Ramirez-Arce, J.L., Monge-Quevedo, A., Lluch-Cota, S.E., 2023. Conversion factors for dry weight for the lion paw scallop (*Nodipecten subnodosus* Sowerby, 1835). Cic. Ocea. 38 (1), 1–7. http://dx.doi.org/10.37543/oceanides.v38i1.283, URL https://www.cicimaroceanides.mx/index.php/revista/article/view/283.

Claereboudt, M.R., Bureau, D., Côté, J., Himmelman, J.H., 1994. Fouling development and its effect on the growth of juvenile giant scallops (*Placopecten magellanicus*) in suspended culture. Aquaculture 121 (4), 327–342. http://dx.doi.org/10.1016/0044-8486(94)90268-2, URL https://linkinghub.elsevier.com/retrieve/pii/0044848694902682.

Cochard, J.C., Devauchelle, N., 1993. Spawning, fecundity and larval survival and growth in relation to controlled conditioning in native and transplanted populations of *Pecten maximus* (L.): evidence for the existence of separate stocks. J. Exp. Mar. Biol. Ecol. 169 (1), 41–56. http://dx.doi.org/10.1016/0022-0981(93)90042-M, URL https://www.sciencedirect.com/science/article/pii/002209819390042M.

Conan, G., Shafee, M.S., 1978. Growth and biannual recruitment of the black scallop *Chlamys varia* (L.) in lanveoc area, Bay of Brest. J. Exp. Mar. Biol. Ecol. 35 (1), 59–71. http://dx.doi.org/10.1016/0022-0981(78)90090-4, URL https://www.sciencedirect.com/science/article/pii/0022098178900904.

Crisóstomo, R.O., Pepe-Victoriano, R., Méndez-Ancca, S., Zambrano-Cabanillas, A.W., Marín-Machuca, O., Perez, H.M., Yana-Mamani, V., Ruiz-Choque, M., 2024. Reproductive conditioning of the Peruvian Scallop *Argopecten purpuratus* in different environments. Fishes 9 (1), 9. http://dx.doi.org/10.3390/fishes9010009, URL https://www.mdpi.com/2410-3888/9/1/9. Number: 1 Publisher: Multidisciplinary Digital Publishing Institute.

Culliney, J.L., 1974. Larval development of the giant Scallop *Placopecten magellanicus* (Gmelin). Biol. Bull. 147 (2), 321–332. http://dx.doi.org/10.2307/1540452, URL https://www.jstor.org/stable/1540452. Publisher: Marine Biological Laboratory.

Davidson, L.-A., 1998. Maturation gonadique de pétoncle géant *Placopecten magellanicus* (Gmelin) du stade juvénile au stade adulte (Ph.D. thesis). Université de Moncton.

DEBtool, 2022. Software package DEBtool_M. URL https://github.com/add-my-pet/DEBtool_M.

Douglas, D.J., Kenchington, E.R., Bird, C.J., Pocklington, R., Bradford, B., Silvert, W., 1997. Accumulation of domoic acid by the sea scallop (*Placopecten magellanicus*) fed cultured cells of toxic *Pseudo-nitzschia multiseries*. Can. J. Fish. Aquat. Sci. 54 (4), 907–913. http://dx.doi.org/10.1139/f96-333, URL http://www.nrcresearchpress.com/doi/10.1139/f96-333.

DuPaul, W., 1970. Natural and ex-vessel moisture content of Sea Scallops (*Placopecten magellanicus*). http://dx.doi.org/10.21220/M2-CJKR-3188, URL https://scholarworks.wm.edu/reports/1630.

DuPaul, W.D., Kirkley, J.E., Schmitzer, A.C., 1989. Evidence of a semiannual reproductive cycle for the sea scallop, *Placopecten magellanicus* (Gmelin, 1791), in the mid-Atlantic region. J. Shellfish Res 8 (1), 173–178.

Farías, A., Uriarte, I., Castilla, J.C., 1998. A biochemical study of the larval and postlarval stages of the Chilean scallop *Argopecten purpuratus*. Aquaculture 166 (1), 37–47. http://dx.doi.org/10.1016/S0044-8486(98)00204-X, URL https://www.sciencedirect.com/science/article/pii/S004484869800204X.

García-Corona, J.L., Hégaret, H., Deléglise, M., Marzari, A., Rodríguez-Jaramillo, C., Foulon, V., Fabioux, C., 2022. First subcellular localization of the amnesic shellfish toxin, domoic acid, in bivalve tissues: Deciphering the physiological mechanisms involved in its long-retention in the king scallop *Pecten maximus*. Harmful Algae 116, 102251. http://dx.doi.org/10.1016/j.hal.2022.102251, URL https://www.sciencedirect.com/science/article/pii/S1568988322000798.

García-Corona, J.L., Hegaret, H., Lassudrie, M., Derrien, A., Terre-Terrillon, A., Delaire, T., Fabioux, C., 2024. Comparative study of domoic acid accumulation, isomer content and associated digestive subcellular processes in five marine invertebrate species. Aquat. Toxicol. 266, 106793. http://dx.doi.org/10.1016/j.aquatox.2023.106793, URL https://www.sciencedirect.com/science/article/pii/S0166445X23003958.

Guillaumot, C., Saucède, T., Morley, S.A., Augustine, S., Danis, B., Kooijman, S.A.L.M., 2020. Can DEB models infer metabolic differences between intertidal and subtidal morphotypes of the Antarctic limpet *Nacella concinna* (Strebel, 1908)? Ecolog. Modell 430, 109088. http://dx.doi.org/10.1016/j.ecolmodel.2020.109088.

Hallegraeff, G.M., Anderson, D.M., Cembella, A.D., Enevoldsen, H.O., 2004. Manual on harmful marine microalgae. 2nd revised edition.. UNESCO, http://dx.doi.org/10.25607/OBP-1370, URL https://repository.oceanbestpractices.org/handle/11329/282. Accepted: 2016-05-05T22:02:34Z ISBN: 9789231039485.

Hallegraeff, G., Enevoldsen, H., Zingone, A., 2021. Global harmful algal bloom status reporting. Harmful Algae 102, 101992. http://dx.doi.org/10.1016/j.hal.2021.101992, URL https://www.sciencedirect.com/science/article/pii/S1568988321000196. Global Harmful Algal Bloom Status Reporting.

Haya, K., Wildish, D.J., 1991. Domoic acid in shellfish and plankton from the Bay of Fundy, New Brunswick, Canada. J. Shellfish Res 10 (1), 113–118.

Heasman, M.P., O'Connor, W.A., Frazer, A.W., Languet, Y., O'Connor, S.J., 2002. Alternative means of nursery culture for commercial scallop (*Pecten fumatus* Reeve) spat. Aquaculture 213 (1), 323–338. http://dx.doi.org/10.1016/S0044-8486(02)00354-X, URL https://www.sciencedirect.com/science/article/pii/S004484860200354X.

Kooijman, B., 2010. Dynamic energy budget theory for metabolic organisation, third ed. Cambridge University Press, http://dx.doi.org/10.1017/CBO9780511805400, URL https://www.cambridge.org/core/product/identifier/9780511805400/type/book.

Kooijman, S.A.L.M., 2014. Metabolic acceleration in animal ontogeny: An evolutionary perspective. Dynamic energy budget theory: Applications in marine sciences and fishery biology, J. Sea Res. Dynamic energy budget theory: Applications in marine sciences and fishery biology, 94 (Supplement C), 128–137. http://dx.doi.org/10.1016/j.seares.2014.06.005.URL http://www.sciencedirect.com/science/article/pii/S1385110114001105,

Kooijman, S.A.L.M., Lika, K., Augustine, S., Marn, N., 2021. Multidimensional scaling for animal traits in the context of dynamic energy budget theory. Conserv. Physiol 9 (1), coab086. http://dx.doi.org/10.1093/conphys/coab086, URL http://dx.doi.org/10.1093/conphys/coab086.

Kvrgić, K., Lešić, T., Džafić, N., Pleadin, J., 2022. Occurrence and seasonal monitoring of domoic acid in three shellfish species from the Northern Adriatic Sea. Toxins 14 (1), 33. http://dx.doi.org/10.3390/toxins14010033, URL https://www.mdpi.com/2072-6651/14/1/33.

Langton, R.W., Robinson, W.E., Schick, D., 1987. Fecundity and reproductive effort of sea scallops *Placopecten magellanicus* from the Gulf of Maine. Marine Ecol. Progr. Ser 37 (1), 19–25, URL https://www.jstor.org/stable/24825487. Publisher: Inter-Research Science Center.

Lavaud, R., Flye-Sainte-Marie, J., Jean, F., Emmery, A., Strand, Ø., Kooijman, S.A., 2014. Feeding and energetics of the great scallop, *Pecten maximus*, through a DEB model. J. Sea Res. 94, 5–18. http://dx.doi.org/10.1016/j.seares.2013.10.011, URL https://linkinghub.elsevier.com/retrieve/pii/S1385110113002116.

Lavaud, R., Kooijman, B., Augustine, S., 2017. *Pecten_maximus*. AmP Collection URL https://www.bio.vu.nl/thb/deb/deblab/add_my_pet/entries_web/Pecten_maximus/Pecten_maximus_res.html.

Le Pennec, M., Paugam, A., Le Pennec, G., 2003. The pelagic life of the pectinid *Pecten maximus*: a review. ICES J. Mar. Sci. 60 (2), 211–233. http://dx.doi.org/10.1016/S1054-3139(02)00270-9, URL https://academic.oup.com/icesjms/article/60/2/211/623789.

Lika, K., Augustine, S., Kooijman, S.A.L.M., 2020. The use of augmented loss functions for estimating dynamic energy budget parameters. Ecol. Model. 428, 109110. http://dx.doi.org/10.1016/j.ecolmodel.2020.109110.

Lika, K., Kearney, M.R., Freitas, V., van der Veer, H.W., van der Meer, J., Wijsman, J.W.M., Pecquerie, L., Kooijman, S.A.L.M., 2011. The "covariation method" for estimating the parameters of the standard dynamic energy budget model I: Philosophy and approach. The AquaDEB project (phase II): what we've learned from applying the Dynamic Energy Budget theory on aquatic organisms, J. Sea Res. The AquaDEB project (phase II): what we've learned from applying the Dynamic Energy Budget theory on aquatic organisms, 66 (4), 270–277. http://dx.doi.org/10.1016/j.seares.2011.07.010.URL https://www.sciencedirect.com/science/article/pii/S1385110111001055,

Liu, H., Kelly, M., Campbell, D., Dong, S., Zhu, J., Wang, S., 2007. Ingestion of domoic acid and its impact on king scallop (*Pecten maximus*, Linnaeus 1758). J. Ocean Univ. China 6, 175–181. http://dx.doi.org/10.1007/s11802-007-0175-6.

Louati, D., BenMiled, S., Saoud, N.B.B., 2020. HermaDEB: An evolutionary IBM for energy allocation in hermaphrodites. Ecol. Model. 424, 109008. http://dx.doi.org/10.1016/j.ecolmodel.2020.109008, URL https://www.sciencedirect.com/science/article/pii/S0304380020300806.

Lubet, P., Devauchelle, N., Muzellec, M., Paulet, Y., Faveris, R., Dao, J.-C., 1995. Reproduction of *Pecten maximus* from different fisheries areas: Rade de Brest, Baie de Saint-Brieuc, Baie de Seine. URL https://archimer.ifremer.fr/doc/00049/15984/.

MacDonald, B.A., Bricelj, V.M., Shumway, S.E., 2016. Chapter 7 - Physiology: Energy acquisition and utilisation. In: Shumway, S.E., Parsons, G.J. (Eds.), Developments in Aquaculture and Fisheries Science. In: Scallops, 40, Elsevier, pp. 301–353. http://dx.doi.org/10.1016/B978-0-444-62710-0.00007-9, URL https://www.sciencedirect.com/science/article/pii/B9780444627100000079.

MacDonald, B.A., Thompson, R.J., 1985. Influence of temperature and food availability on the ecological energetics of the giant scallop *Placopecten magellanicus*. Reproductive output and total production. Mar. Ecol. Progr. Ser 25, 295–303.

MacDonald, B.A., Thompson, R.J., 1986. Influence of temperature and food availability on the ecological energetics of the giant scallop *Placopecten magellanicus*. Mar. Biol 93, 37–48.

MacDonald, B.A., Thompson, R.J., 1988. Intraspecific variation in growth and reproduction in latitudinally differentiated populations of the giant Scallop *Placopecten magellanicus* (Gmelin). Biol. Bull. 175 (3), 361–371. http://dx.doi.org/10.2307/1541727, URL https://www.journals.uchicago.edu/doi/10.2307/1541727.

Maeda-Martínez, A.N., Lodeiros-Seijo, C., 2011. Biología y cultivo de los moluscos pectínidos del género *Nodipecten*, 1a ed Centro de Investigaciones Biológicas del Noroeste, Limusa, México, D.F., OCLC: 820570783.

Mafra Jr., L.L., Bricelj, V.M., Ouellette, C., Léger, C., Bates, S.S., 2009. Mechanisms contributing to low domoic acid uptake by oysters feeding on *Pseudo-nitzschia* cells. I. Filtration and pseudofeces production. Aquatic Biol. 6, 201–212. http://dx.doi.org/10.3354/ab00121, URL https://www.int-res.com/abstracts/ab/v6/p201-212/.

Maldonado-Amparo, R., Ramírez, J.L., Ávila, S., Ibarra, A.M., 2004. Triploid lion-paw scallop (*Nodipecten subnodosus* Sowerby); growth, gametogenesis, and gametic cell frequencies when grown at a high food availability site. Aquaculture 235 (1–4), 185–205. http://dx.doi.org/10.1016/j.aquaculture.2003.12.014, URL https://linkinghub.elsevier.com/retrieve/pii/S0044848603008421.

Marques, G.M., Augustine, S., Lika, K., Pecquerie, L., Domingos, T., Kooijman, S.A.L.M., 2018. The AmP project: Comparing species on the basis of dynamic energy budget parameters. PLoS Comput. Biol. 14 (5), e1006100. http://dx.doi.org/10.1371/journal.pcbi.1006100, URL https://journals.plos.org/ploscompbiol/article?id=10.1371/journal.pcbi.1006100. Publisher: Public Library of Science.

Marques, G.M., Lika, K., Augustine, S., Pecquerie, L., Kooijman, S.A.L.M., 2019. Fitting multiple models to multiple data sets. Ecosystem based management and the biosphere: a new phase in DEB research, J. Sea Res. Ecosystem based management and the biosphere: a new phase in DEB research, 143, 48–56. http://dx.doi.org/10.1016/j.seares.2018.07.004.URL https://www.sciencedirect.com/science/article/pii/S1385110117303441,

Martínez, G., Pérez, H., 2003. Effect of different temperature regimes on reproductive conditioning in the scallop *Argopecten purpuratus*. Aquaculture 228 (1), 153–167. http://dx.doi.org/10.1016/S0044-8486(03)00321-1, URL https://www.sciencedirect.com/science/article/pii/S0044848603003211.

Mauriz, A., Blanco, J., 2010. Distribution and linkage of domoic acid (amnesic shellfish poisoning toxins) in subcellular fractions of the digestive gland of the scallop *Pecten maximus*. Toxicon 55 (2), 606–611. http://dx.doi.org/10.1016/j.toxicon.2009.10.017, URL https://www.sciencedirect.com/science/article/pii/S0041010109005066.

Mazon-Suastegui, J.M., Maeda-Martínez, A.N., Robles-Mungaray, M., De La Roche, J.P., Rupp, G., Mendes-De-Bem, M., Velasco, L.A., Freites-Valbuena, L.F., 2011. Avances en la produccion de juvenukes de *Nodipecten* spp.. In: Biología y cultivo de los moluscos pectínidos del género *Nodipecten*, 1a ed Centro de Investigaciones Biológicas del Noroeste, Limusa, México, D.F., OCLC: 820570783.

Meer, J.v.d., Donk, S.v., Sotillo, A., Lens, L., 2020. Predicting post-natal energy intake of lesser black-backed gull chicks by dynamic energy budget modeling. Ecolog. Modell 423, 109005.

Minchin, D., 2003. Introductions: some biological and ecological characteristics of scallops. Aquat. Living Resour. 16 (6), 521–532. http://dx.doi.org/10.1016/j.aquliv.2003.07.004, URL https://linkinghub.elsevier.com/retrieve/pii/S0990744003000937.

Navarro, J.M., Leiva, G.E., Martinez, G., Aguilera, C., 2000. Interactive effects of diet and temperature on the scope for growth of the scallop *Argopecten purpuratus* during reproductive conditioning. J. Exp. Mar. Biol. Ecol. 247 (1), 67–83. http://dx.doi.org/10.1016/S0022-0981(00)00140-4, URL https://www.sciencedirect.com/science/article/pii/S0022098100001404.

Parsons, G.J., Robinson, S.M.C., Chandler, R.A., Davidson, L.A., Lanteigne, M., Dadswell, M.J., 1992. Intra-annual and long-term patterns in the reproductive cycle of giant scallops *Placopecten magellanicus* (Bivalvia: Pectinidae) from Passamaquoddy Bay, New Brunswick, Canada. Mar. Ecol. Progr. Ser 80 (2/3), 203–214, URL https://www.jstor.org/stable/24826607. Publisher: Inter-Research Science Center.

Paulet, Y., Lucas, A., Gerard, A., 1988. Reproduction and larval development in two *Pecten maximus* (L.) populations from Brittany. J. Exp. Mar. Biol. Ecol. 119 (2), 145–156. http://dx.doi.org/10.1016/0022-0981(88)90229-8, URL https://linkinghub.elsevier.com/retrieve/pii/0022098188902298.

Pazos, A.J., Román, G., Acosta, C.P., Abad, M., Sánchez, J.L., 1997. Seasonal changes in condition and biochemical composition of the scallop *Pecten maximus* L. from suspended culture in the Ria de Arousa (Galicia, N.W. Spain) in relation to environmental conditions. J. Exp. Mar. Biol. Ecol. 211 (2), 169–193. http://dx.doi.org/10.1016/S0022-0981(96)02724-4, URL https://www.sciencedirect.com/science/article/pii/S0022098196027244.

Pecquerie, L., Johnson, L.R., Kooijman, S.A.L.M., Nisbet, R.M., 2011. Analyzing variations in life-history traits of Pacific salmon in the context of dynamic energy budget (DEB) theory. J. Sea Res. 66, 424–433.

Perodou, D., Latrouite, D., 1981. Contribution à l'étude de la reproduction du pétoncle noir (*Chlamys varia*) de la baie de Quiberon. URL https://archimer.ifremer.fr/doc/00021/13260/.

Pousse, E., Flye-Sainte-Marie, J., Alunno-Bruscia, M., Hégaret, H., Rannou, E., Pecquerie, L., Marques, G.M., Thomas, Y., Castrec, J., Fabioux, C., Long, M., Lassudrie, M., Hermabessiere, L., Amzil, Z., Soudant, P., Jean, F., 2019. Modelling paralytic shellfish toxins (PST) accumulation in *Crassostrea gigas* by using dynamic energy budgets (DEB). J. Sea Res. 143, 152–164. http://dx.doi.org/10.1016/j.seares.2018.09.002, URL https://linkinghub.elsevier.com/retrieve/pii/S1385110118300339.

Priol, E., 1930. La coquille saint-jacques (*Pecten maximus*), résumé de nos connaissances pratiques sur ce mollusque. Revue des Travaux de l'Institut des Pêches Maritimes 3 (2), 143–173, URL https://archimer.ifremer.fr/doc/00000/5853/. Publisher: ISTPM.

Purce, D.N., Donovan, D.A., Maeda-Martínez, A.N., Koch, V., 2020. Scope for growth of cultivated Pacific and Gulf of California populations of lion's paw scallop *Nodipecten subnodosus*, and their reciprocal transplants. Lat. Am. J. Aquat. Res. 48 (4), 538–551. http://dx.doi.org/10.3856/vol48-issue4-fulltext-2468, URL http://lajar.ucv.cl/index.php/rlajar/article/view/vol48-issue4-fulltext-2468.

R. core team, 2022. R: a language and environment for statistical computing. R foundation for Statistical computing, Vienna, Austria, URL https://www.R-project.org/.

Racotta, I.S., Ramirez, J.L., Ibarra, A.M., Rodríguez-Jaramillo, M.C., Carreño, D., Palacios, E., 2003. Growth and gametogenesis in the lion-paw scallop *Nodipecten* (*Lyropecten*) *subnodosus*. Aquaculture 217 (1), 335–349. http://dx.doi.org/10.1016/S0044-8486(02)00366-6, URL https://www.sciencedirect.com/science/article/pii/S0044848602003666.

Ramírez Arce, J.L., 2009. Evaluación de la ventaja productiva y grado de esterilidad en triploides de almeja mano de león *Nodipecten subnodosus* (Sowerby 1835) como una alternativa para el cultivo en el Parque Nacional Bahía de Loreto, Golfo de California (Ph.D. thesis). Instituto Politécnico Nacional. Centro Interdisciplinario de Ciencias Marinas, URL http://www.repositoriodigital.ipn.mx//handle/123456789/13928. Accepted: 2013-02-26T23:46:43Z.

Régnier-Brisson, L., 2024. Ecologie et dynamique de la croissance du pétoncle noir (*Mimachlamys varia*) en Rade de Brest (Ph.D. thesis). Université de Bretagne occidentale - Brest, URL https://theses.hal.science/tel-04700195.

Ren, J.S., 2009. Effect of food quality on energy uptake. Metabolic organization: 30 years of DEB applications and developments, J. Sea Res. Metabolic organization: 30 years of DEB applications and developments, 62 (2), 72–74. http://dx.doi.org/10.1016/j.seares.2008.11.002.URL https://www.sciencedirect.com/science/article/pii/S1385110108001299,

REPHYTOX, 2023. REPHYTOX dataset. French monitoring program for Phycotoxins in marine organisms. Data since 1987. French Monitoring Program For Phycotoxins In Marine Organisms, http://dx.doi.org/10.17882/47251, URL https://www.seanoe.org/data/00361/47251/. Type: dataset.

Roddick, D.L., Lundy, M.J., Kenchington, E., 1994. Yield per recruit analysis and minimum meat weight recommendations for the bay of Fundy Scallop Fishery. DFO Atlantic Fisher. Res. Document 94/58, 15.

Saavedra, C., Peña, J.B., 2006. Phylogenetics of American scallops (Bivalvia: Pectinidae) based on partial 16S and 12S ribosomal RNA gene sequences. Mar Biol 150 (1), 111–119. http://dx.doi.org/10.1007/s00227-006-0335-z, URL http://dx.doi.org/10.1007/s00227-006-0335-z.

Sauvey, A., Denis, F., Hégaret, H., Le Roy, B., Lelong, C., Jolly, O., Pavie, M., Fauchot, J., 2021. Interactions between filter-feeding bivalves and toxic diatoms: Influence on the feeding behavior of *Crassostrea gigas* and *Pecten maximus* and on toxin production by *Pseudo-nitzschia*. Toxins 13 (8), 577. http://dx.doi.org/10.3390/toxins13080577, URL https://www.mdpi.com/2072-6651/13/8/577. Number: 8 Publisher: Multidisciplinary Digital Publishing Institute.

Serrano-Guzmán, S., Robles-Mungaray, Velasco-Blanco, Voltolina, D., Chairez, H., 1997. Larval culture of Mexican pectinids *Argopecten ventricosus* (circularis) (Sowerby 1842) and *Lyropecten subnodosus* (Sowerby 1835) in a commercial hatchery. Centro Interdisciplinario de Ciencias Marinas.

Shafee, M.S., 1981. Seasonal changes in the biochemical composition and calorific content of the black scallop *Chlamys varia* (L.) from Lanvéoc, Bay of Brest. Oceanol. Acta 4 (3), 331–342.

Shafee, M., Lucas, A., 1982. Variations saisonnières du bilan énergétique chez les individus d'une population de *Chlamys varia* (L.) : Bivalvia, Pectinidae. Oceanol. Acta 5 (3), 331–338, URL https://archimer.ifremer.fr/doc/00120/23171/. Publisher: Gauthier-Villars.

Shumway, S.E., Parsons, G.J., 2016. Scallops: Biology, Ecology, Aquaculture, and Fisheries. Elsevier, Google-Books-ID: vhGdBAAAQBAJ.

Stechele, B., Maar, M., Wijsman, J., Van der Zande, D., Degraer, S., Bossier, P., Nevejan, N., 2022. Comparing life history traits and tolerance to changing environments of two oyster species (*Ostrea edulis* and *Crassostrea gigas*) through dynamic energy budget theory. Conserv. Physiol. 10 (1), coac034. http://dx.doi.org/10.1093/conphys/coac034, URL http://dx.doi.org/10.1093/conphys/coac034.

Stotz, W.B., González, S.A., 1997. Abundance, growth, and production of the sea scallop *Argopecten purpuratus* (Lamarck 1819): bases for sustainable exploitation of natural scallop beds in north-central Chile. Fish. Res. 32 (2), 173–183. http://dx.doi.org/10.1016/S0165-7836(97)00010-6, URL https://www.sciencedirect.com/science/article/pii/S0165783697000106.

van der Veer, H.W., Cardoso, J.F.M.F., van der Meer, J., 2006. The estimation of DEB parameters for various Northeast Atlantic bivalve species. Dynamic Energy Budgets in Bivalves, J. Sea Res. Dynamic Energy Budgets in Bivalves, 56 (2), 107–124. http://dx.doi.org/10.1016/j.seares.2006.03.005.URL https://www.sciencedirect.com/science/article/pii/S1385110106000451,

Villalejo-Fuerte, Arellano-Martínez, M., Robles-Mungaray, M., Ceballos-Vázquez, B.P., 2004. Notes on the growth, survival, and reproduction of the lion's paw scallop *Nodipecten subnodosus* maintained in a suspended culture. Hidrobiológica 14 (2), 161–165, URL https://www.scielo.org.mx/pdf/hbio/v14n2/v14n2a10.pdf.

Wohlgeschaffen, G.D., Mann, K.H., Subba Rao, D.V., Pocklington, R., 1992. Dynamics of the phycotoxin domoic acid: accumulation and excretion in two commercially important bivalves. J Appl Phycol 4 (4), 297–310. http://dx.doi.org/10.1007/BF02185786, URL http://link.springer.com/10.1007/BF02185786.

Wright, J.L.C., Boyd, R.K., Freitas, A.S.W.d., Falk, M., Foxall, R.A., Jamieson, W.D., Laycock, M.V., McCulloch, A.W., McInnes, A.G., Odense, P., Pathak, V.P., Quilliam, M.A., Ragan, M.A., Sim, P.G., Thibault, P., Walter, J.A., Gilgan, M., Richard, D.J.A., Dewar, D., 1989. Identification of domoic acid, a neuroexcitatory amino acid, in toxic mussels from eastern Prince Edward Island. Can. J. Chem. 67 (3), 481–490. http://dx.doi.org/10.1139/v89-075, URL http://www.nrcresearchpress.com/doi/10.1139/v89-075.